Feasibility Analysis of Subsea Pumped Hydro Storage Plant

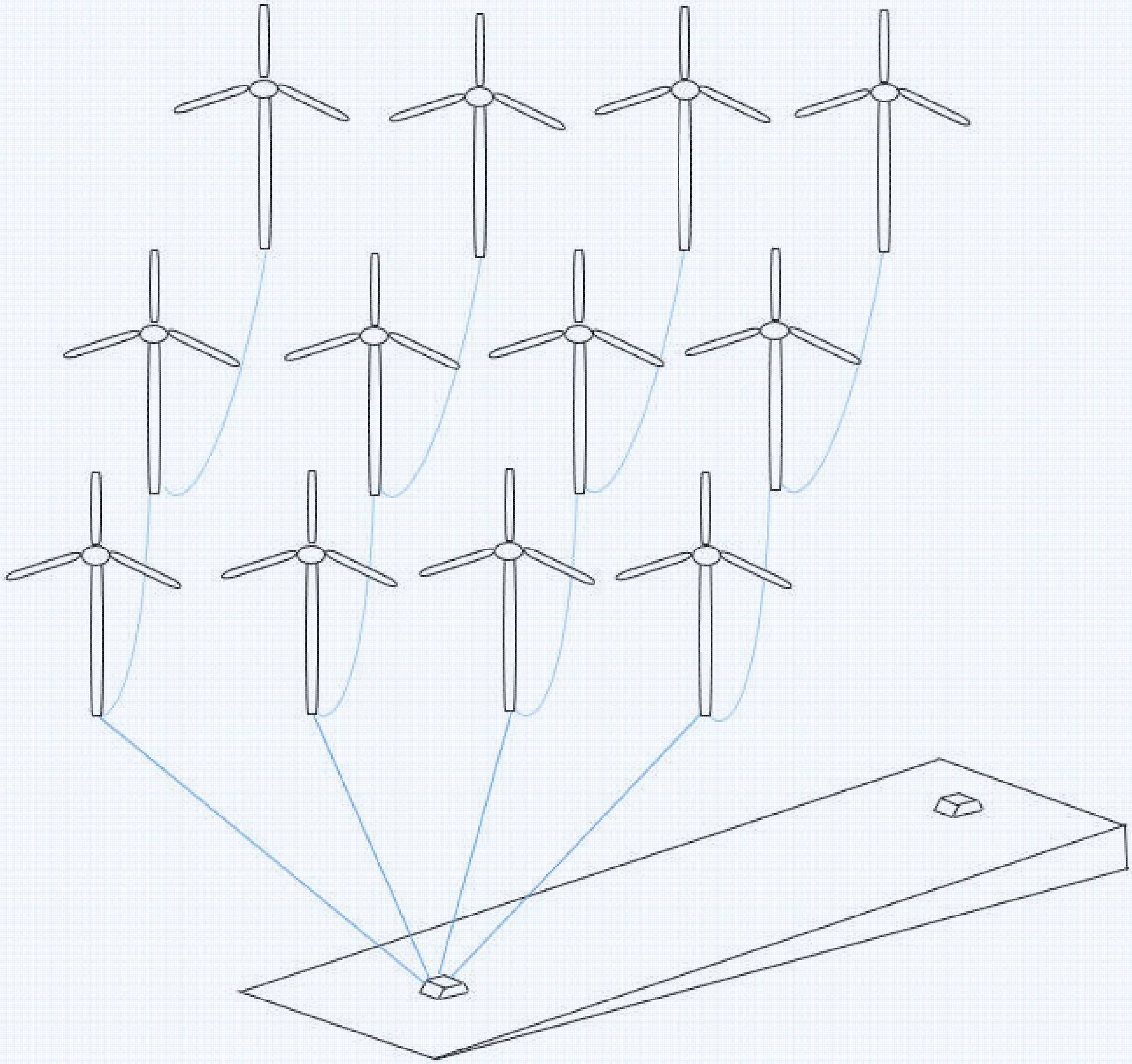

Vineet Arya

Feasibility Analysis of Subsea Pumped Hydro Storage Plant

By

Vineet Arya

in partial fulfilment of the requirements for the degree of

Master of Science
in Offshore and Dredging Engineering

at the Delft University of Technology,
to be defended publicly on Monday November 15, 2021 at 11:00 AM.

Thesis committee:	Dr. Sape Andries Miedema	TU Delft
Supervisor :	Dr. Antonio Jarquin Laguna	TU Delft
	Ir. Rasmus Julin	SubSea 7
	Ir. Ernst Kloster	SubSea 7

Preface

This report presents my graduation work to conclude my Master Offshore & Dredging at the Delft University of Technology. The topic of this research is the Feasibility Analysis of the Subsea Pumped Hydro Storage Plant. The study was carried out in collaboration with Subsea 7. This feasibility study elucidates the design of an energy storage facility from the conceptual idea up to the preliminary design.

First and foremost, I would want to thank the members of my graduation committee which include Dr. Sape Andries Miedema, Dr. Antonio Jarquin Laguna, Ir. Rasmus Julin, & Ir. Ernst Kloster for their assistance during this research endeavor. I'd want to express my gratitude to Antonio Jarquin Laguna and Rasmus Julin for their detailed input following each meeting. I am grateful for their insights gained via several constructive conversations and comprehensive feedback, which assisted me in steering this thesis in the right path.
Secondly, I want to express my sincere thanks to all of my family members, especially my wife Anu, for their unwavering support during the completion of this project.

Vineet Arya

Contents

Abstract

Renewable energy sources, such as wind energy, are gaining a lot of traction across the world. India intends to improve the amount of wind energy integration into the national electricity system. Wind/solar energy's major drawback is its inherent changeability and source unpredictability, making it a challenging resource to dispatch.

A proposed PHS system known as Subsea Pumped Hydro Storage (SPHS) has been assessed from a techno-economic standpoint. As intermittent renewable energy sources become increasingly widespread in the electrical system, the demand for power regulation grows. Implementing energy storage in the system is one approach to balance the demand for power with the supply. This thesis looked at an idea that is a sea-based variant of the existing pumped hydro storage technique. A SPHS unit is made up of a hollow structure on the seabed that may be emptied of water using a pump during periods of low demand and high energy generation in the system, and the unit is charged at that moment. When the system requires more energy, water is permitted to flow into the tank through a turbine, creating power.

In India, a locality study of prospective areas where the PHS may be placed and operated effectively is carried out. Muppandal (Tamil Nadu) is used as a case study. When the PHES is used, a positive influence on the power system's behavior may be seen, with the degree of wind integration being raised and dispatched on demand. The generation of peak demand by inefficient and costly units is reduced, lowering the total generating cost.

The main goal of this work is to determine the Technical feasibility of a proposed SPHSP system and to evaluate Levelised cost of storage. The study will be conducted to reach out to the suitable selection of turbines and pumps and to design the concrete storage tank in such a deep-sea environment. It is observed that the maximum depth upto which the storage tank can be built is 1200m depth for 5m high wall and 1000m depth for 7m high wall. The appropriate turbine is selected based on specific speed and it comes out that Francis turbine is suitable for depth 200m to 1200m. The levelised cost of storage (LCOS) is also calculated, and it works out to be $4.53 per kilowatt hour for 1200m depth. There are different methods suggested to increase the bearing capacity of the soil and compaction grouting seems to be the most appropriate improvement method.

LIST OF FIGURES

LIST OF TABLES

LIST OF ABBREVIATIONS

Pumped Hydro Storage	: PHS
Subsea Pumped Hydro Storage Plant	: SPHSP

LIST OF NOMENCLATURES

Q_P	:	Rated volume flow rate (m^3/s)
P_P	:	Rated Pump Power (watt)
η_p	:	Pump efficiency
ρ	:	Density of water ($1000 Kg/m^3$).
g	:	Acceleration due to gravity (9.8 m/s^2).
Ns	:	Specific speed (RPM)
T	:	Rated pumping time in second
h	:	Head (m)
η_P	:	Pump efficiency
V_R	:	Volume of the upper reservoir (m^3)
η	:	Turnaround efficiency of PHES
H_s	:	Static head (m)

1.0 Introduction

1.1 Renewable Energy Overview

Near the water, more than half of the world's population lives(Pazheri et al., 2014). Fourteen of the world's seventeen major cities are located on the coast. Current trends in global urbanization indicate that this tendency will continue. The placement of electricity generation as near to consumption as feasible is a key concept of energy distribution. Long transmission costs money and decreases the efficiency of the energy system.

Offshore natural resources provide enormous potential for renewable energy development. Offshore energy generating also avoids the problems of limited space and human sensory closeness. The sea's energy abundance manifests itself in a variety of ways. Its sun, wind, waves, currents, and thermoclines provide well-known energy harvesting options. However, marine engineering has always been a high-stakes, high-cost sport. Aside from that, one of the most significant problems that the terrestrial variations of these generating potential confront is dispatchability.

Energy from renewable sources becoming more prevalent. Many countries across the world have begun to construct facilities that generate electricity using renewable energy sources. The relevance of renewable energy sources is highlighted by the climate change issues posed by the excessive usage of fossil fuels.

Economic impacts, energy security, and CO2 emission reduction are three major motivators for the advancement of renewable energy systems. Technology advancements have enabled countries to produce renewable energy more cost effectively.

After hydropower, wind energy is one of the most viable and dependable renewable energy technologies (Power Technology, 2020). Wind energy technology has advanced in recent years, resulting in a rise in investment projects. Wind energy, unlike fossil fuels, is long-term and environmentally friendly. The cumulative impacts on the environment are considerably less serious than those of nonrenewable energy sources.

Typically, wind farms are connected to the electric utility transmission network. This farm produces variable electricity that is relatively consistent year after year but varies significantly over short time periods, affecting the grid's performance.

As a result, there is a pressing need to incorporate storage devices into the power system, which aid in the in controlling the movement of electricity in the electric grid.

1.2 Renewable Energy in India

India has significant renewable energy potential, such as solar and wind, and it aspires to be one of the first countries to participate in the renewable energy sector's development.

It is certain that the wind energy offshore business in India will continue to grow as it has 7800 km long coastal length. Pumped hydroelectric energy storage (PHES) in the deep sea is one of the systems that can be used for energy storage and load balancing as an alternative. They provide auxiliary services at high ramp rates, and they may also benefit from daily energy price variations by discharging energy during peak demand hours and using it to pump water into a high potential energy reservoir during off-peak periods.

1.3 Problem statement

There are several technical challenges with the offshore wind.

- The offshore wind farm with water depth greater than 150m generates huge amount of electricity. This energy can be used to meet the peak load demand. However, during night when demand is low this energy gets wasted in absence of the storage system.
- The variations in the wind become a major challenge to the stability of the transmission systems and the security of supply for the customer.
- With ever increase in fuel prices and mounting environmental concerns, the energy from renewable resources, particularly wind energy is becoming hugely popular throughout the world (IRENA, 2017). As the peaker plant can be replaced with PHS and thus dependency on fuel is getting reduced.

Thus the above concerns greatly motivate the adoption of proposed SPHSP System integration. The major challenge with the SPHSP is that it cannot be built to a depth more than 1200 m because of the high hydrostatic pressure on the structure. Another challenge is to choose suitable pump & turbines for such greater depths.

1.4 The main objectives

The main goal of this research is to determine the technical feasibility of a proposed PHS system and to evaluate the levelised cost of storage for a particular case scenario in India. To check the feasibility, the following objectives of the thesis shall be assessed.

- Sizing and the preliminary design of the subsea storage tank.
- Suitable selection of pump and turbines
- Simplified economic analysis regarding the levelised cost of storage

1.5 Methodology

The study will be carried out in two parts. The first part will deal with technical aspects of the proposed project, which commences with determining how much power storage is required to meet the peak demand. The required grid data was obtained from the government official website that Tamil Nadu Electricity Board (TANGEDCO, 2017) that is responsible for the distribution of the energy to Tamil Nadu. Once the energy demand is obtained, this energy demand will be used as an input to define the boundary conditions on the required energy storage and power for this particular case study. The study will be conducted to reach out to the suitable selection of turbines and pumps and to design the concrete storage tank in a deep-sea environment. Based on the energy demand the structural sizing is finalized and then the design of the tank will be carried out by using the relevant codes. The second part will deal with the simplified economic analysis regarding the Levelised cost of storage (LCOS) and know what would be a cost-effective demand.

The project also comprises the development of the numerical tool in python/excel to design the subsea pumped hydro storage tank. The input for the tool will be field parameters such as meteorological and geological/geotechnical data and available excess energy data. The output of the numerical tool will be a storage tank. The current thesis will use the data of Muppandal (Tamil Nadu) to study the technical feasibility of the proposed concept.

1.6 Thesis layout

The thesis will be divided into 9 chapters.

Ch:1 presents the background of the study, the problem statement, objectives and its methodology.

Ch:2 represents literature that are published on different topics relevant to the study.

Ch:3 include the configuration & the design aspects of new PHS.

Ch:4 represents the classification and selection of Pump and Turbines.

Ch:5 represents the analysis of the levelized cost of storage of new PHS.

Ch:6 & Ch:7 covers other technical aspects such as Soil improvement & Constructability.

Ch:8 & Ch:9 include the conclusions and provides some recommendations.

2.0 Literature Review

The function and utility of energy storage in electrical networks that are anticipated to absorb growing amounts of time variable power output from renewable sources are examined. India, with its huge renewable energy potential, receives special attention. Energy storage ideas span a broad range of stages of development, from mature technologies like pumped hydro, which has more than 50 years of operating experience, to newer technologies like hydrogen storage systems and flow batteries, which are currently in research.

Energy storage has the potential to play a variety of roles in the functioning of power systems. The following are the most important:

1. Dealing with intermittency caused by the integration of time-variable renewable generating sources, resulting in enhanced decarbonization of the power supply system.
2. Providing solutions in grid constrained areas.
3. Assisting with energy security.
4. Operational cost savings and financial/commercial prospects.

The major disadvantages of these sorts of storage facilities include the unique siting difficulties that arise for each unit because they all need to be totally custom-made based on location, as well as the significant environmental and demographic consequences they have. These challenges, taken together, necessitate the development of a sea-based energy storage technology that does not compete for space with other sectors of society.

2.1 India on Renewable Energy Path

The Indian government has set goals to achieve a low-carbon economy by 2030, including generating at least 40% of the country's energy needs from renewable sources(IRENA, 2017). Energy storage will certainly increase supply security and reliability, allowing present and future energy demands to be met within the current national grid system. Figure 1 shows that by 2030 there is tremendous increase of renewable energy and which ultimate demands into increase of pump hydro storage plants.

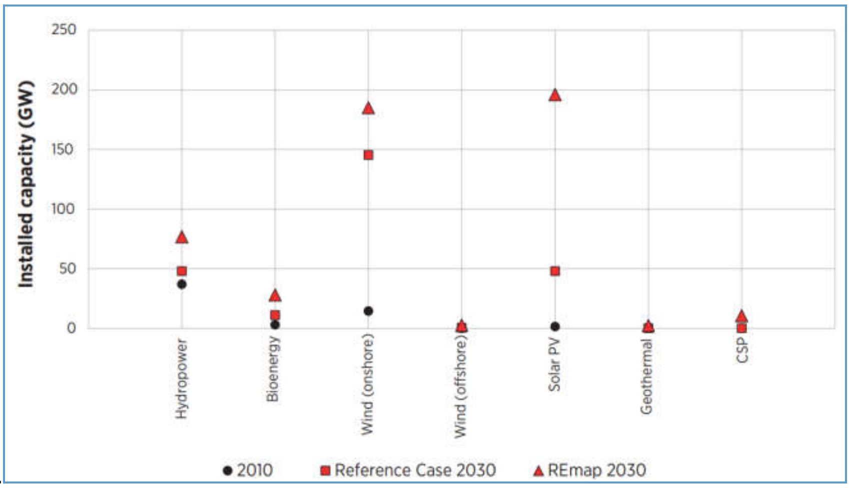

Figure 1 Renewable power capacity developments
Image taken from (IRENA, 2017)

Reference Case 2030 : The country's present policies and plans.

REmap – Renewable Energy Roadmaps/prospects for India
The International Renewable Energy Agency (IRENA) has developed a roadmap to 2030 (REmap) to explore different energy technology options, highlighting ways to increase the uptake of renewable energy beyond the country's present policies and plans. IRENA's REmap programme determines the potential for countries, regions and the world to scale up renewables.
The Indian government believes that Power storage may play an important and rising role alongside renewable electricity supply in addressing the intermittency of some kinds of renewable output.

Potential Benefits of Increased Use of PHS

•Enabling the most efficient use of existing generation, particularly renewable energy sources.
• Less reliance on fossil fuel plants for backup power.
• Using stored energy to improve power quality and prevent transitory network limitations, storage helps to stabilize the transmission and distribution system
• Advantages for generators who can store power at low prices and sell it at higher prices.
• The possibility of reducing greenhouse gas emissions; and
• The ability to provide 'black start' capacity through storage capacity.

Renewable energy continues to make inroads into the Indian electricity sector. Traditionally, peak demand for energy has been met by boosting fossil fuel output. However, in a system with a high renewable penetration, this method may not be the best option. Unlike traditional plants, sustainable power advances are less able to adapt to variations in demand. Energy storage, as a supplemental source of power generation, has the potential to increase supply security and reliability, aiding in fulfilling current and anticipated energy demands.

By 2022, India wants to construct 175 GW of renewable energy capacity. By 2030, Figure 2, India's overall energy consumption will have more than doubled, with electricity demand nearly tripling (IRENA, 2017). India's overall gross power capacity would more than double by 2030, from 284 gigawatts (GW) in 2015 to an estimated 670 GW, with annual electricity output more than tripling from 1100 terawatt-hours (TWh) to around 3450 TWh (IRENA, 2017). By 2030, the country has the ability to provide 10% of the global CO2 emission reduction potential from renewable energy (IRENA, 2017).

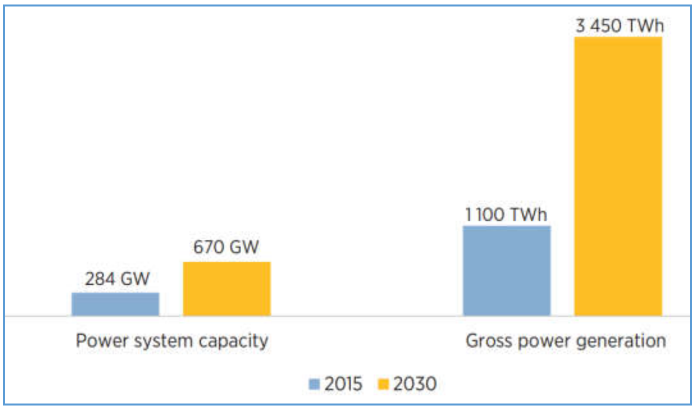

Figure 2 Power system capacity and generation, 2015-2030
Image taken from (IRENA, 2017)

2.2 History of PHES

In the recent decade, interest in massive Electrical Energy Storage (EES) systems has exploded as a viable solution to many of the problems associated with renewable energy. When compared to traditional fossil fuel power production, one of the most important problems of many low-carbon generation systems is that they lack the same level of load-following flexibility. This is true for renewable energy systems that are affected by weather. Primary energy resources such as wind and sun, for example, are diverse and frequently surprising.
One of the most critical issues that bulk EES attempts to address is the restricted capacity of wind and solar systems to load-follow. Many research studies have identified energy storage as a critical component of the flexibility required to incorporate large amounts of renewable energy into power networks.

According to a paper prepared for the National Renewable Energy Laboratory by Denholm et al., 2010 large penetrations of variable generation will increase interest in all flexibility alternatives, including energy storage devices. Beaudin et al., 2010 conclude that large-scale renewables integration would be an extra tough task without energy storage.

Cochran et al., 2012 examine the best ways for integrating variable renewable power into the grid, concluding that there is no one-size-fits-all solution. As a result, the development of energy storage technologies will be aided. Although it is well acknowledged that lower percentages of renewable energy may be incorporated into many electrical power networks without causing significant operational changes (Gross et al., 2007).

PHES also has a number of benefits throughout the power supply chain, which have been discussed in certain research papers (Barbour et al., 2016a). These include:

- Enabling more low-carbon generation deployment
- Facilitating time-of-use energy management
- Increasing end-user reliability
- Minimizing electricity price fluctuations
- Improving system reliability
- Maximizing system flexibility
- Reducing the need for transmission upgrades/new transmission infrastructure
- Reducing overall pollutant emissions

PHES stores electrical energy by raising water to the upper reservoir, as depicted in Figure 3. By using the excess power to pump water from a lower reservoir to a higher reservoir, the charging process transforms electrical energy into mechanical energy and, eventually, gravitational potential energy. The discharge process transforms gravitational potential energy into mechanical energy, which is subsequently converted to electrical energy, by allowing water to flow down from the higher reservoir to the lower reservoir, driving a turbine connected to an electrical generator.
At a country level, China has the most PHS installed capacity, at 30.32 GW (Zhu & Ma, 2019). Japan has the second-largest PHS capacity, followed by the United States. However, PHS accounts for just 1.8 percent and 1.9 percent of their total installed electric generation capacity, respectively. Table 1 lists some of the nations with the most PHS capacity deployed and it shows China and Japan has the highest number of PHS followed by USA. Table 1 shows Installed PHES capacity by country and current (2020) capacity under construction (• *Global Pumped Storage Hydropower Capacity 2020 | Statista*, n.d.)

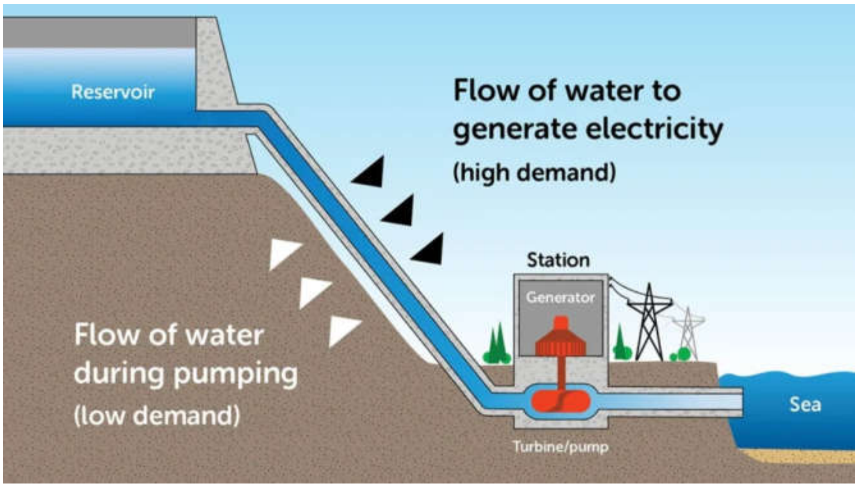

Figure 3 PHES Operation
Image Taken from (ARUP, 2020)

Table 1 Installed PHES capacity by country and current (2020) capacity under construction

Country	Installed PHS capacity (GW)	Under construction (GW)
China	30.32	60
South Africa	2.7	1
Germany	5.35	1.4
Italy	3.94	-
India	4.78	3.15
Japan	21.89	2.82
USA	19.14	52.48
Spain	3.32	2.6
South Korea	4.7	-
United Kingdom	2.6	1.73

2.3 Historical development of PHES

India

The 770 MW Nagarjunasagar facility, which was fully operational in 1981, was India's first pumped storage plant. Another 742 MW of PHES was built between 1981 and 1998, followed by another 3450 MW between 2003 and 2008 (Barbour et al., 2016b). The need to satisfy peak electrical demand is the primary incentive for building PHES in India; peak power capacity in most states falls short of peak demand by 10-15%. Pumped hydro facilities are designed to move power from off-peak to peak hours(Sivakumar et al., 2013).

After China, the United States, and Germany, India has the fourth biggest installed capacity in wind power(*Top 10 Countries in Wind Energy Capacity | REVE News of the Wind Sector in Spain and in the World*, n.d.). India has a 7600-kilometer-long coastline(*Offshore Wind | Ministry of New and Renewable Energy, Government of India*, 2021). Muppandal in Figure 4 is a candidate location in India (Tamil Nadu). It is India's largest wind farm. It has 3000 wind turbines with a cumulative installed capacity of 1500 MW (*Muppandal (India) - Wind Farms - Online Access - The Wind Power*, n.d.). Between May and September, the average speed in Tamil Nadu is 12-13 m/s. (Carolin Mabel & Fernandez, 2008). The average annual wind speed is 5-6 m/s. (Carolin Mabel & Fernandez, 2008). This shows there is an ample potential for wind energy in India especially in the southern part of the country.

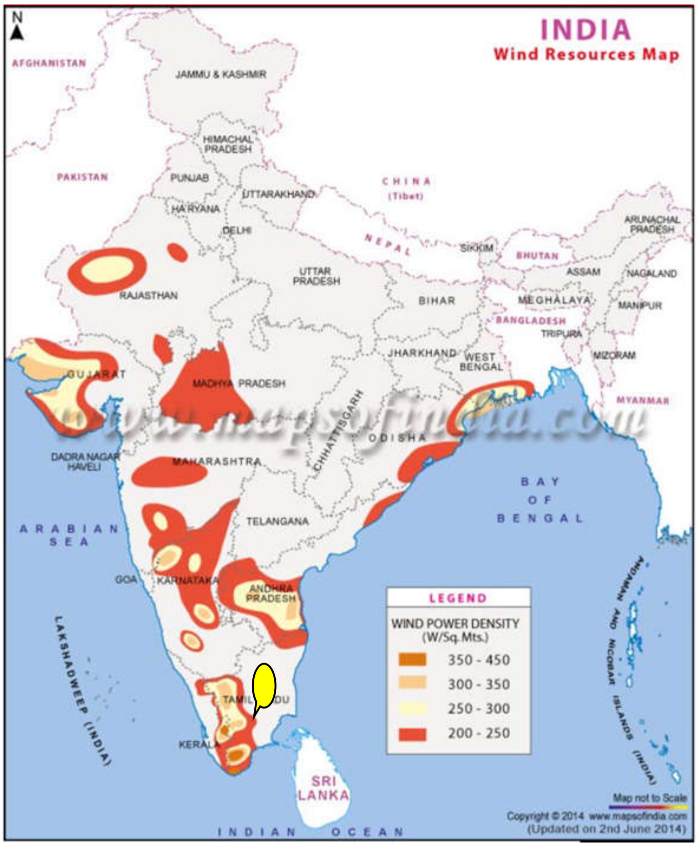

Figure 4 India Wind Map

Image taken from Source:(*Wind Resources in India*, n.d.)

Europe

European nations have the largest PHES capacity, with more than 80% of it being built between 1960 and 1990. The majority of the systems are located in Germany, Italy, France, Spain, and Switzerland's hilly areas. Although, in a number of countries, development occurred along with large expansions in nuclear power capacity (Barbour et al., 2016b). Even without nuclear power, several countries, like Austria, installed substantial PHES capacity. The yearly percentage rate of PHES development in European nations has grown somewhat since 2008, which is considered to be a response to rising energy demand in the 1990s and the anticipated of greater wind output. Some of Europe's newest PHES initiatives include the 430 MW Reisseck II system in Austria (commissioned in 2014) and the 852 MW extension of the Spanish La Muela pumped storage facility(Barbour et al., 2016a).

China

In comparison to Europe, the United States, and Japan, China's PHES development was comparatively recent. The first PHES scheme (11 MW) was built in 1968, followed by the second in 1975. After thereafter, expansion slowed until the 1990s (Barbour et al., 2016b). For a variety of causes, it has grown rapidly since then. With

China's rapid economic expansion, demand for electricity has risen. In addition to increasing grid dependability, PHES may be considered to be extremely beneficial in bridging the valley-to-peak gap.
Regional carbon reduction objectives and the fast expansion of wind energy in North and West China, along with a lack of transmission infrastructure, are also seen as key drivers for PHES development(Zeng et al., 2013) At the end of 2013, China has 91.4 GW of installed wind capacity (Barbour et al., 2016c).
China's significant proportion of coal-based power generation is another push for more flexible generation. Because most plants are big scale (> 300 MW), less efficient, and less cost-effective to run at partial load (Barbour et al., 2016c). The growth of PHS capacity coincides with large increases in traditional hydro generating capacity (Barbour et al., 2016c)

USA

The majority of PHES stations in the United States were built between 1960 and 1990. Significant gains in nuclear capacity occurred during this time period (Barbour et al., 2016b). According to (Deane et al., 2010), considerable rises in the cost of crude oil and gas in the 1970s, along with uncertainty about future pricing, led utilities in the United States to consider PHES as an alternative to fossil fuel peaking units. More recently, with lower power price ranges for PHES stations than for traditional peaking units, PHES was frequently more economically appealing.
As a consequence of subsequent declines in the price of oil and gas, as well as substantial cuts in the capital costs of Combined Cycle peaking units, there has been limited deployment of PHES in the United States since 1990. According to some studies, the United States has a PHES potential of more over 1000 GW(Yang & Jackson, 2011).
Taum Sauk, Yards Creek, Muddy Run, and Cabin Creek were all part of the contemporary pumped storage era in the United States, which began in the mid-1960s.

Japan

Japan has built PHES systems in the past to supplement its nuclear power and give an alternative to fossil fuel peaking units. Japan has chosen nuclear power as its major source of electricity generation (Barbour et al., 2016b). Japan has constructed a substantial capacity of PHES systems to supplement its nuclear power and offer peak electricity for energy security concerns. Furthermore, it lacks any electrical links with neighboring countries (unlike France, for instance, which is a significant exporter of nuclear-generated power in the United Kingdom, Germany, Italy, Switzerland and Spain). This increases the value of flexible producing plants and helps to explain why the percentage of PHES capacity in the Philippines is much greater than in many other nations. Although the bulk of the most appropriate locations have been built, Japan's hilly terrain is ideal for PHES installations(Anuta et al., 2014).
The following sections cover those types of energy storage considered to be viable, and include short descriptions of how the technology works, unit sizes available and associated costs. The different types of storage technology are categorized as: mechanical; electrical; and chemical storage.

2.4 New advancement in the field of Pumped Hydro Storage.

Pumped hydro, Subsea Pumped Hydro Storage (SPHS), and The Stensea System are the three types covered here.

2.4.1 Pumped Hydro

Pumped hydroelectricity storage is the most widely used large-scale power storage technique due to its low cost. Water flow is utilized to create or release stored energy into the system in this kind of mechanical energy storage. Pumped hydro is, in general, the most developed technology of the different energy storage options, with the lowest prices per unit of stored electricity. A significant portion has already been installed.

The following is the general operational flow of pumped hydro. Water is pumped to a reservoir at a higher elevation using electricity. When there is a need for energy, the water is transported through a series of turbine generators to a lower reservoir, where the mechanical energy of the water is converted to electrical energy, which is then delivered into the grid. The two ways of operation for pumped hydro are shown in Figure 5.

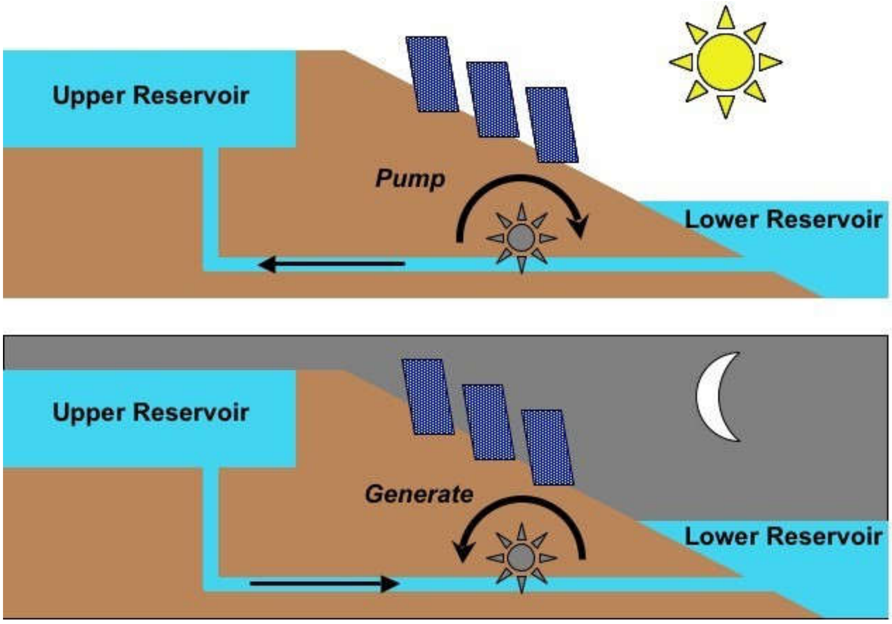

Figure 5 Pumped Hydro Flow
Image taken from (Infield & Hill, 2014)

Pumped hydro storage is mostly viewed as long-term storage due to its size and the amount of time it may be used. It has discharge windows that can last up to 10 hours. As a result, it may be utilized to significantly lower peak loads on the electrical grid. To do this, the system will typically pump water to the upper reservoir during low demand (and therefore low cost) periods, then release the water during high demand (and thus high cost) intervals, reducing the peak load that must be met by traditional plant. It may significantly increase the load factor of other plants in the power system by doing so.

There are a considerable number of operating projects and related documentation regarding the possibilities of this technology, partly owing to the maturity of the technology. The energy storage capacity of a pumped hydro storage facility is in the GWh range, with power ratings ranging from hundreds of MW to about 1–2 GW. Pumped hydro storage has an average efficiency of approximately 75%, however some projects have achieved efficiencies of up to 80% (Infield & Hill, 2014). Pumped hydro storage also has a significantly longer lifespan than most other kinds of energy storage. If properly maintained, the civil works will endure virtually indefinitely, while the turbines and generators will last many decades.

Pumped hydro storage offers both advantages and disadvantages in terms of the environment. The obvious benefit is the possibility to reduce the usage of fossil fuel generation by lowering the requirement for peaking units that rely on fossil fuels to generate electricity. Siting – finding a place for both reservoirs might be challenging – and building, which can have long-term consequences on the ecosystem, are both issues.

Because of the lengthy equipment lives of well over 10,000 cycles, most projects are able to repay their expenses. This is significantly superior to other storage methods now available. Table 2 below shows the costs,(Infield & Hill, 2014)

Table 2 Pumped Hydro Storage Costs (Infield & Hill, 2014)

	Maturity	Capacity (MWh)	Power (MW)	Duratioı (hrs)	Round Trip efficiency (%)	Lifetime (Cycles)	Total cost ($/kW)	Cost ($/kWh)
Grid support (ancillary services) and integration of intermittent renewables								
Small Pumped Hydro	Mature	1,680-5,300	280-530	6-10	80-82	>13,000	2,500-4,300	420-430
Large Pumped Hydro	Mature	5,400-14,000	900-1,400	6-10	80-82	>13,000	1,500-2,700	250-270

Construction prices vary considerably based on location, which is an important aspect to consider when calculating these costs. Costs on the ground may differ substantially from those listed above.

Traditional pumped hydro is replaced with seawater pumped hydro, which uses the sea as the lower water reservoir. This allows for greater site flexibility, but capital costs are likely to be higher due to the need for corrosion protection in the pump. Additional costs may be incurred in order to build a suitable higher storage reservoir. Only one of these systems, a 30 MW plant in Japan, has been installed thus far. The extensive coastline of Scotland should provide opportunities for this technology, but no full study of the technology's potential has been done so far. The cost-effectiveness of the installation increases as the height of the sea cliffs increases. Because of its proximity to the shore, this type of storage might be a useful complement to marine renewable energy output.

Another form is underground pumped hydro, which uses caverns or abandoned mines as the lower reservoir and a lake as the upper reservoir (or even the sea). They must be regarded as speculative at this time because no systems have been built or full cost estimates have been provided.

2.4.2 Subsea Pumped Hydro Storage (SPHS)

A novel energy storage system known as Subsea Pumped Hydro Storage (SPHS) has been assessed from a techno-economic standpoint. As intermittent renewable energy sources become increasingly widespread in the electrical system, the demand for power regulation grows. Implementing energy storage in the system is one approach to balance the demand for power with the supply. This thesis looked at an idea that is a sea-based variant of the existing pumped hydro storage technique.

A SPHS unit is made up of a hollow structure on the seabed that may be emptied of water using a pump during periods of low demand and high energy generation in the system, and the unit is charged at that moment. When the system requires more energy, water is allowed to flow back into the cavity through a turbine, creating power.

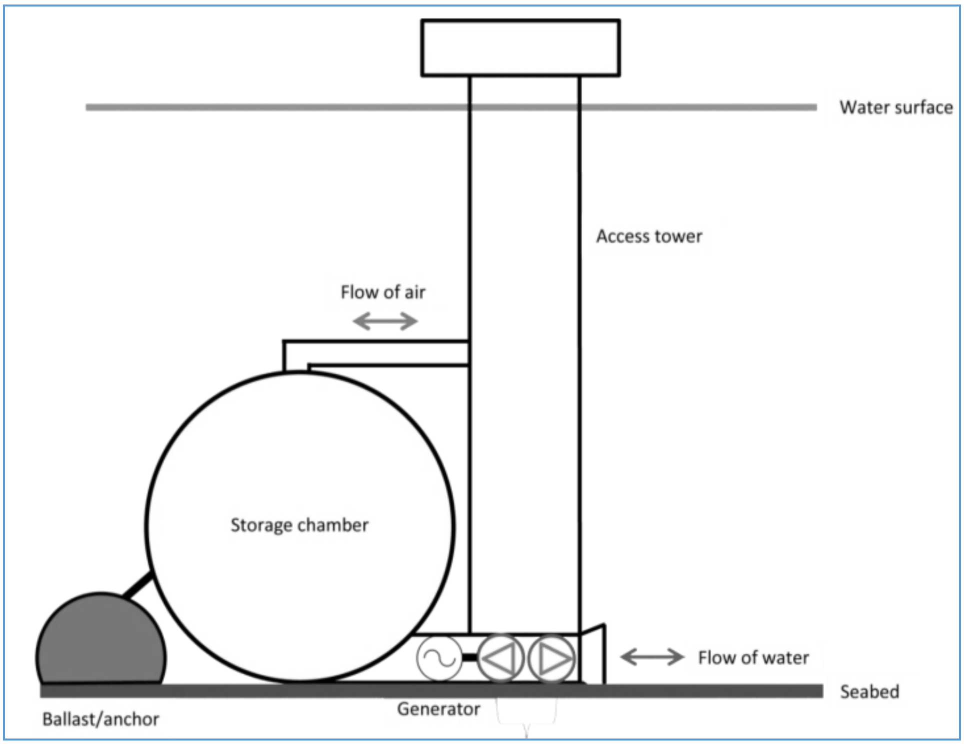

Figure 6 Subsea Pumped Hydro Storage
Image taken from (Falk, 2013)

2.4.3 The Stensea SyStem

It will be required to extend the grid and enhance storage capacity in order to convert the electrical system to a renewable energy system. Currently, and in the future, pumped hydro energy storage systems are the most common way to store extra energy. The selection of suitable and conflict-free areas for the growth of conventional pumped hydro energy systems on land is a key problem.

The development of an offshore pumped hydro storage idea, which was tested for the first time in the project StEnSEA (Storing Energy at Sea) at the Fraunhofer Institute for Energy Economics and Energy Systems

Technology IEE (previously IWES Kassel), might enable the utilization of new sites at sea. The key need for this innovative technique is enough water depth at a short distance from the coast. The StEnSEA project conducted a thorough system analysis with the creation of the design, construction, and logistics concept based on a feasibility assessment. The pump turbine unit has also been examined, as well as its integration with the storage system.
In addition, the innovative offshore storage systems' integration into the energy grid has been studied, and a techno-economic evaluation has been conducted in order to establish a roadmap for their technological implementation. The installation of a 1:10 size prototype, which was successfully tested in the winter of 2016 in Lake Constance, was a key aspect of the project. Aside from its enormous global potential, another major feature of the offshore pumped hydro storage system is that the system's power may be changed depending on the number of units put in a facility. This opens up a variety of operational ideas for the offshore pumped hydro storage system, perhaps paving the way for this new technology to become a significant element of the future energy supply.
Instead of the well-known standard pumped-hydro power plants, which require two independent water reservoirs of various heights, the StEnSea concept uses the static pressure of the water column in deep seas. To make advantage of its potential, a hollow concrete sphere is built in deep water. A pump-turbine is housed within the hollow sphere, allowing energy to be stored. Energy may be stored as water flows into the sphere. When the water pours into the sphere, the store is empty. The pump-turbine is generating power in turbine mode in this example. To re-charge the storage system, water is forced out of the sphere against the pressure of the surrounding water column. A schematic cross sectional depiction of an energy storage sphere is shown in Figure 7

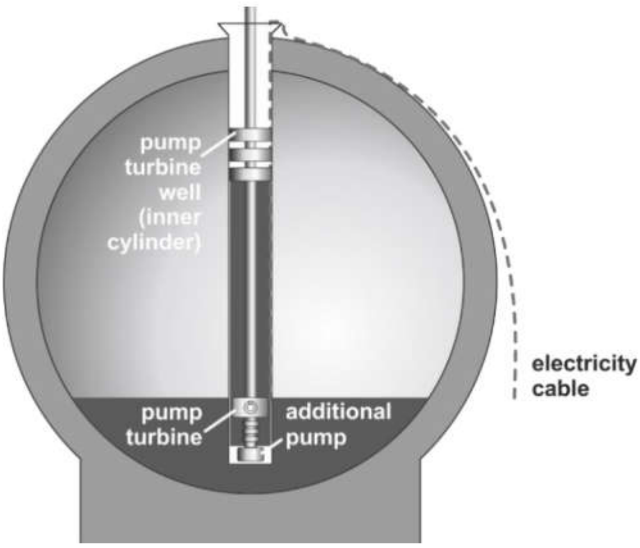

Figure 7 Stensea
Image taken from (*Storing energy at sea*, 2016)

2.6 Advantages of PHS for Wind Integration

The following are some of the advantages of incorporating wind power into the electrical power system: 1. Total generating costs are lowered since conventional plants use far less fuel, and 2. Carbon emissions are reduced because less fossil fuel is consumed (United State Environmental Protection Agency, 2018). Expanded wind power integration, on the other hand, may have a negative influence on the power system's consistency due to the natural unpredictability of wind. These negative consequences can lead to an increase in the cost of maintaining the same degree of power system dependability, which is referred to as wind integration cost. It is critical to identify such negative consequences in order to ensure that only a small portion of the benefits are lost. Many national/international research on combining PHES with wind farms as a way to mitigate wind inconsistency issues are available. As a result of these scientific investigations, several PHS benefits related to wind power integration are mentioned below.

PHES is generally aligned with wind farms in order to make a profit. Instead of selling their electricity to the grid, wind farms can be utilized to pump water from a tank when energy costs are low. When the cost of energy exceeds a certain threshold, the stored water is released back into the tank to create power, which is then sold to the grid. During periods of high energy costs to the grid, wind power is generally sold out.
The use of PHS to manage wind energy variability is becoming more popular across the world. Many research have been conducted to integrate wind power with PHS. All of these studies demonstrate that combining PHS with the power system has substantial benefits.

2.7 Ancillary Services

Pumped storage was originally intended to use power at night to move water from a lower reservoir to a higher reservoir. During the daily peaking hours, when water is returned from the higher to the lower reservoir, power is generated.
PHS projects were designed to assist major base-load nuclear or coal-fired plants by absorbing surplus power generated during off-peak hours and supplying stored energy during on-peak hours from the 1960s through the 1980s.
With the deregulation of the electricity market and the establishment of spot markets, the usage of pumped storage projects has grown significantly over time to include a variety of auxiliary advantages such as load following, spinning reserve, frequency control, and voltage regulation. The next sections go through these technological characteristics and benefits.

2.7.1 Load Following

PHS projects, like traditional hydropower projects, can swiftly follow load demand in the generating mode, whether demand is dropping or growing. In a major power system, morning and evening load fluctuations are generally in the thousands of MW range. To keep up with the load, a number of units must be initiated and shut down on a daily basis. The practice of daily shutdowns of cycle units results in additional operating and

maintenance expenditures due to wear and tear. PHS initiatives minimize the number of start-ups and shutdowns while lengthening the time it takes for other units to start up and shut down.
Conventional PHS projects cannot change their pumping load needs in the pumping mode, thus they are generally run at no load or maximum load. This constraint does not exist with a variable speed PHS project, which may be tweaked throughout a load range of 50 to 60% of rated pumping power (Sant & Thakare, 2019). This would make it easier to integrate wind power.

2.7.2 Frequency Regulation

To balance electricity supply and demand in any power system, the regulating frequency is necessary. On generating units, there are speed governors that are employed to keep a constant eye on frequency. To help balance demand and supply and maintain a consistent frequency, speed governors regulate the unit's power output. The power output, on the other hand, does not alter quickly. The output of a generator can be reduced or raised depending on the kind of generator. Large coal or nuclear units are often slow to alter outputs, but hydro and PS plants are quite responsive.
With the aid of the wicket gates, the governor controls unit speed and frequency in a traditional PSH single speed machine (adjustable guide vanes surround the turbine and control the area available for water to enter the turbine). In less than 10 seconds, these wicket gates may close and open (Gustafsson, 2013).
In both producing and pumping modes, adjustable speed machines can provide frequency control. There are two different types of control components. The first is the turbine governor, which controls the turbine's wicket gate position, and the second is the inverter, which controls the generator/rotor motor's currents.
The reaction rate of an adjustable speed machine is faster than that of a typical unit controlled by a speed governor.

2.7.3 Spinning Reserve

Spinning reserve is another auxiliary function that is critical to any power system. It's the backup generation capacity that can swiftly respond to a sudden loss of imported electricity or a producing unit. In the generating mode, to offer spinning reserve PS projects are occasionally run at a lower capacity than they should be. The potential spinning reserve capability of PS projects is divided into two parts: (i) I spinning reserve in generation mode, when a PS project's generation is less than full capacity, and (ii) spinning reserve in pumping mode, when PS units pumping loads can be instantly stopped.
Because spinning reserve may be plentiful in the system during off-peak hours, spinning reserve in pumping mode for a PS project may not be of significant financial benefit. In the generating mode, an adjustable speed machine has a larger operating zone, while in the pumping mode, it provides spinning reserve capability.

2.7.4 Voltage Control

Voltages and frequencies must be within design limits. Voltage regulation is the process of balancing power supply and demand, but it also includes regulating reactive power, which is measured in VARs (Volt-Ampere

Reactive Power), rather than power. When there is an imbalance in supply and demand, VARs cause voltage to rise or fall across the power system. In both pumping and generation modes, a voltage regulator is utilized to regulate the voltage that is part of the excitation system. Through the excitation framework, the machine voltage is adjusted by altering the field current.

2.7.5 A black start

This is a way for recovering a power transmission system that has been temporarily or completely lost owing to the breakdown of a grid-connected power producing plant. This power plant, which has been disconnected from the grid, will require an electrical source to restart. Not all power plants are capable of supplying electricity from their own power plants, and must instead rely on other sources such as diesel generators. A Pumped Hydro Storage plant may store a reserve of potential energy in the higher reservoir for use only when a black start event happens. This reserve might also be utilized to restart a power plant.

3.0 Configuration and Design of SPHSP

3.1 Configuration of Subsea Pump Hydro Storage tank

An initial configuration of Subsea pumped hydro storage plant is provided by Subsea 7 as shown in Figure 8. The shape of the structure is such that the turbines are installed on the one side of the tank and on another side pumps can be installed. This is a conceptual sketch and in order to make it feasible, it has to be divided into chambers. The intermediate wall needs to be build inside the tank at regular intervals in order to break the span of top and bottom slab. In the current case the tank is divided into four chambers as shown in Figure 9 section A-A. And in order to allow the water to flow from one chamber to another chamber the cutouts in the wall are provided. This will allow the water to pass from one chamber to another chamber. The cut-out on the intermediate walls are shown in Figure 10 section B-B.

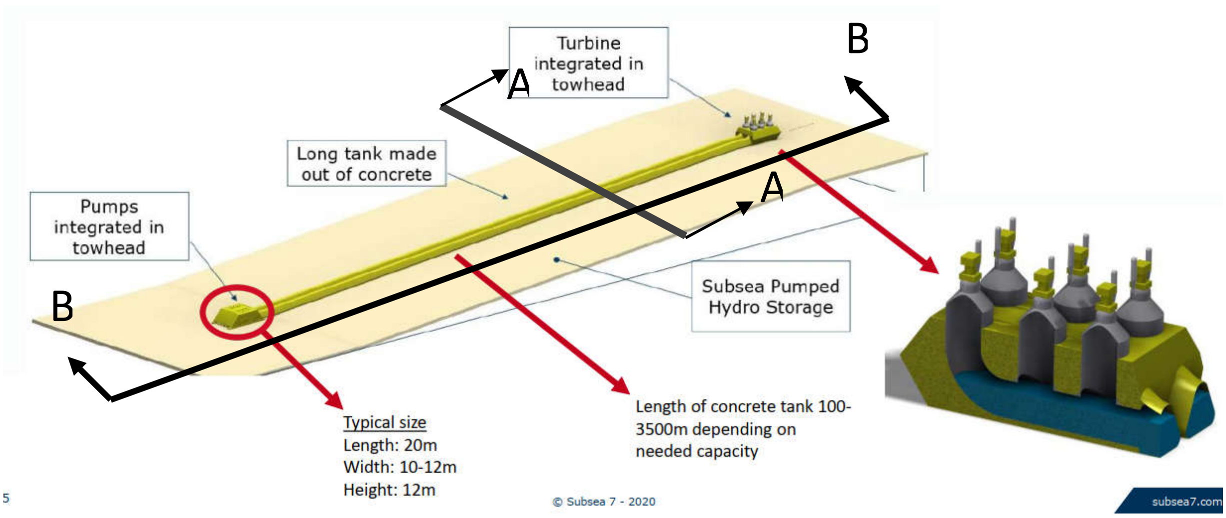

Figure 8 Isometric View of SPHSP
Image taken from Subsea Proposal Document

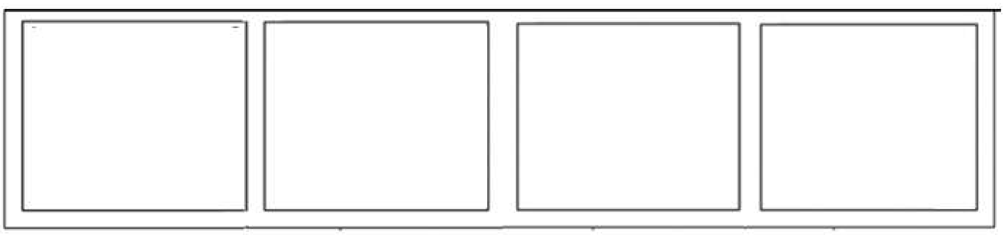

Figure 9 Section A-A of SPHSP

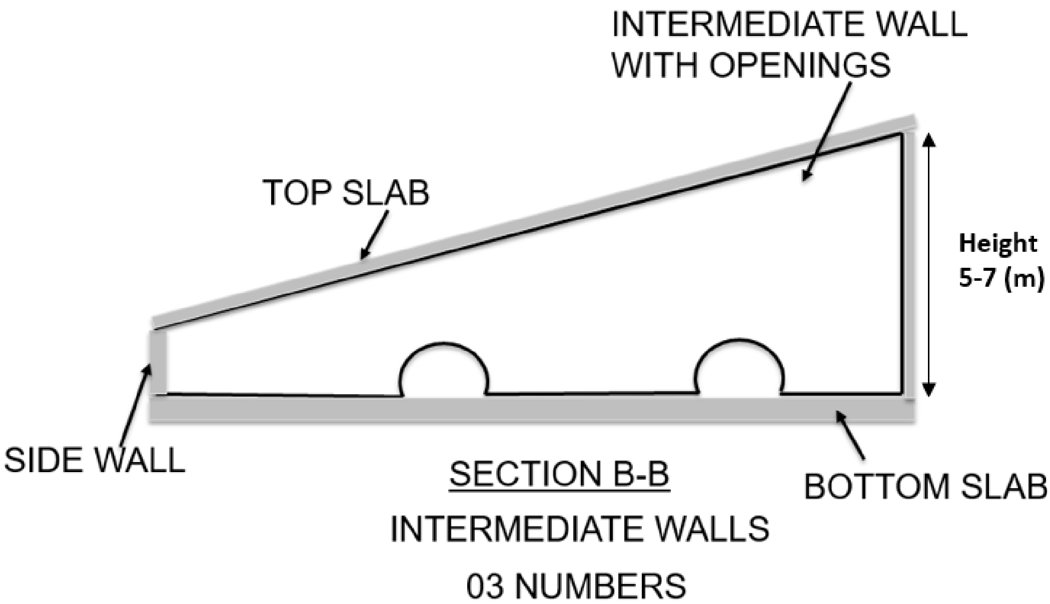

Figure 10 Section B-B of SPHSP

The design of the tank will be performed in five steps. First from the electricity demand, the volume of tank is determined. Secondly, loading from pumps and turbines to be applied along with the high hydrostatic pressure. After the application of the loads the structure is analysed with moment distribution method. This method provides the moment at various section of the structure and which is then used to determine the thickness of the tank. Once the structure is designed then the results are presented in the graphical informs in the subsequent sections.

3.1.1 Volume Determination

To meet the peak hour load demand, Tamil Nadu has to purchase 550 MW of electricity from another state. *[https://www.tangedco.gov.in/linkpdf/installedcapacity(281220).pdf]*. The volume of the tank required to generate 550 MW for the three hours as shown in Figure 10a (Buckley et al., 2019) is given by equation

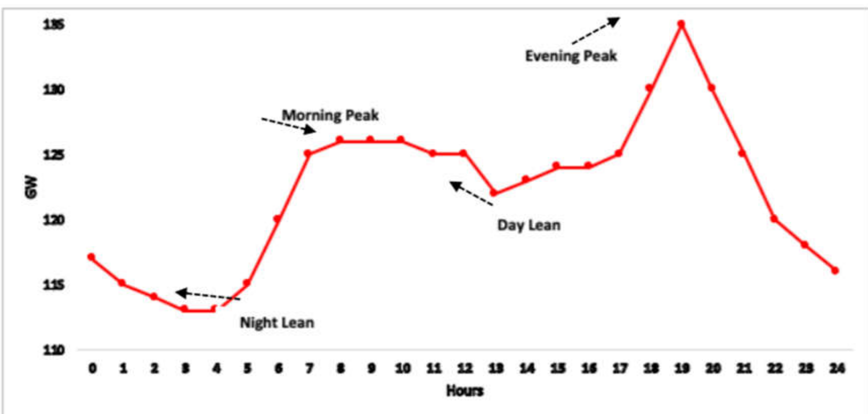

Figure 10a Peak Value vs Power

(1)

$V_R = Q_p \times T$

Where
V_r : Volume of the Tank
Qp: Rated volume flow rate (m^3/s)
T : Rated pumping time in second

$$Q_P = \frac{P_P \times \eta_P}{g \times \rho \times h} \qquad (2)$$

P_p: Rated Pump Power (W)
n_p: Pump efficiency
g: Acceleration of gravity ($9.8 m/s^2$)
ρ : Density of water ($1000 Kg/m^3$)
h: Head (m)

3.1.2 Loading:

The Figure 11 shows the application and type of loading on the tank. The vertical loads acting on cross section are

i) Self-weight of the slab (kN/m) = Thickness of slab x 1 m x unit weight of concrete
ii) Water hydrostatic pressure (kN/m) = Top of tank from sea surface x unit weight of water
iii) Turbine loading of 300 kN (Thapar, 2015)
iv) Base pressure due to vertical load and buoyancy.

Once the loads are applied, the structure is then analysed using the numerical tool developed in excel and is attached as attachment 2. The structure is analysed and designed for the worst scenario where there all turbine loading is acting on the cross-section.

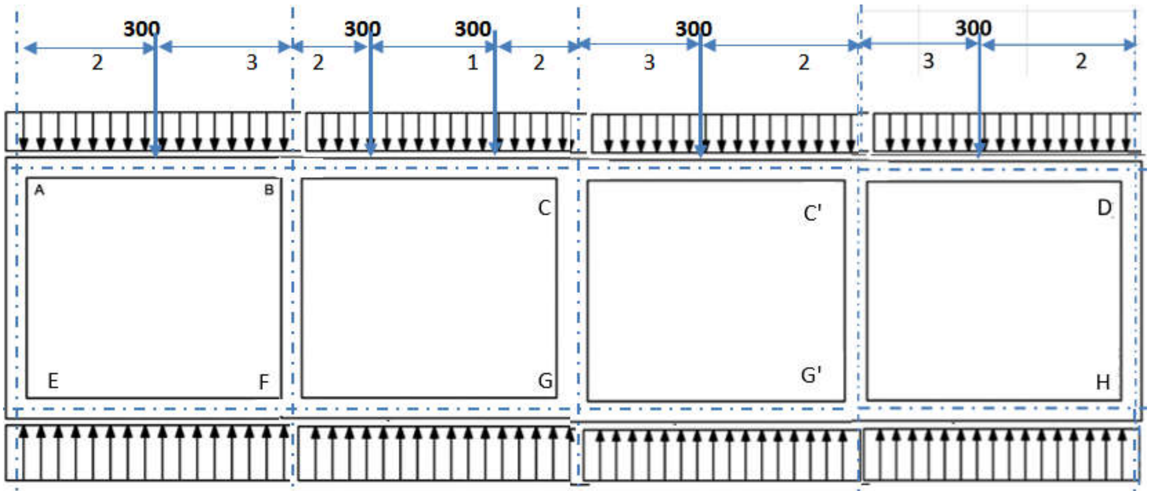

Figure 11 Loading Diagram Include Self weight, Water Pressure, Pump Loading, Base Pressure

The Figure 12 shows the lateral loading on the sides of the wall due to water pressure. The lateral pressure is specific weight of water (kN/m^3) multiplied with height from the water surface. There will be no water pressure on intermediate walls as net water pressure will cancel out each other.

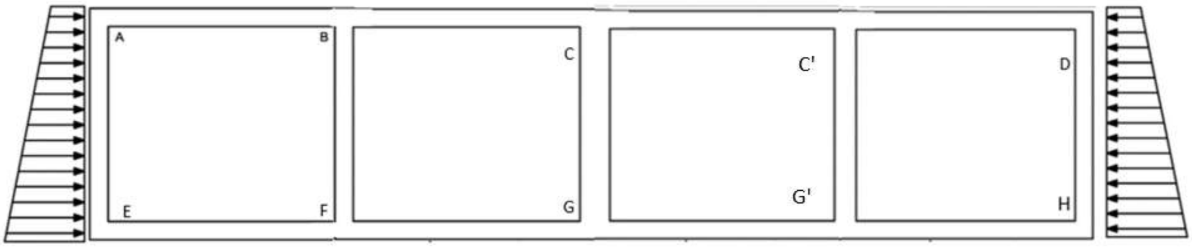

Figure 12 Loading Diagram for Lateral Water pressure

3.1.3 Analysis & Design

The verical and lateral load on the structure results into moment and shear diagram as shown in Figure 12a and 12b. These diagram shows how moment and shear distributed in the structure. In a wall/slab, the internal force system consist of a shear force and a bending moment acting on the cross section. Once these parameters are known across any cross-section then the required thickness and area of steel required at that section can be found.

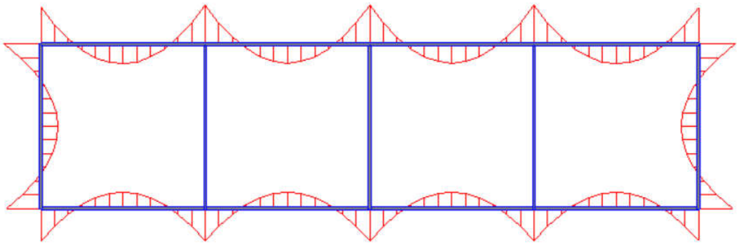

Figure 12a Moment Distribution Diagram

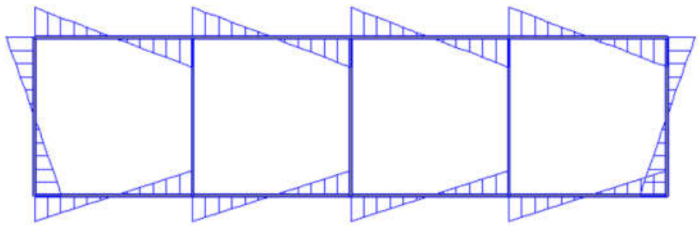

Figure 12b Shear Force Diagram

3.1.4 Shear Strength Check

Shear is the force that causes two contiguous portions of the same body to slide relative to each other in a plane parallel to their contact plane. The stress required to yield or fracture a material in the plane of its cross-section is known as shear strength.

Shear reinforcement is required if the actual shear stress exceeds the allowable shear stress of the concrete employed. Shear reinforcement is used to avoid shear failure and enhance beam ductility, lowering the risk of abrupt failure.

Nominal Shear Stress τ_v = $$\frac{V_u}{bd} \quad (4)$$

Percentage of Tension Reinforcement (P_t %) = $$\frac{Ast \times 100}{bd} \quad (5)$$

Design Shear Strength of Concrete τ_c corresponding to Nominal Shear Stress and percentage of Tension reinforcement. (Refer P.73 table 19 of IS 456 200)

If $\tau_v < \tau_c$ No Shear reinforcement required

If $\tau_v > \tau_c$ Shear Reinforcement required in the form of stirrups

Spacing of Stirrups Sv = $$\frac{0.87 \times fy \times Asv \times d}{Vus} \quad (6)$$

Vus = $$Vu - \tau_c xbxd \quad (7)$$

V_u = Factored Shear force

b = breadth of wall/slab (1000 mm)

d = Thickness of wall/slab

A_{sv} = Area of the stirrups

f_y = yield strength of the reinforcement bar

Area of Steel obtained as Ast = $$\frac{M_u}{d_{eff} \times 0.9 \times f_y} \quad (8)$$

M_u = Factored Moment

d_{eff} = Effective depth

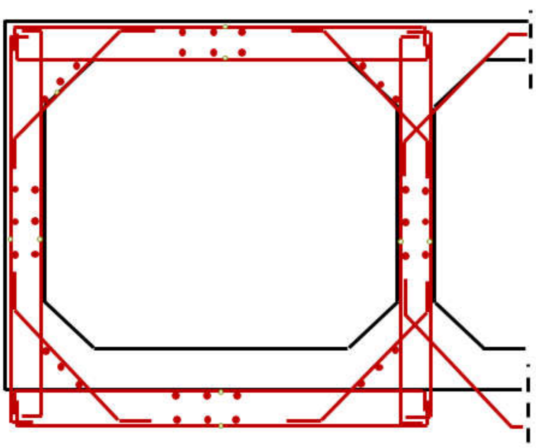

Typical Reinforcement Cross Section

Figure 13 Typical Reinforcement Cross section

To determine stress on any cross-section the shear forces on that section is computed and then divided by the area over which the shear force is acting and it is called nominal shear stress given by equation 4. Due to forces the bending stress is developed in the section and to resist the bending, reinforcement is provided in that section and is given by equation 8. Thus the percentage of reinforcement provided in section is given by equation 5. Concrete has its own shear capacity as well due to the reinforcement in that section (of Indian Standards, n.d.). If the nominal shear force acting on the structure exceeds the total shear capacity of concrete section then additional reinforcement is required and it is provided in terms of stirrups. Thus the spacing of the stirrups provided in the section is given by equation 6.

3.1.5 Results

In this section the results derived from subsection 3.1.2 to 3.1.4 are represented in the graphical form. The graphs for moments, cross section thickness and overall cost are shown with respect to the depth. The moment distribution method has been used to evaluate the moments at different cross section of the structure. Once moment at any cross section is obtained then the thickness of that section is obtained using equation 8 of subsection 3.1.4. The graphs so obtained from the analysis represent how these three parameters vary as we go deeper into the sea.

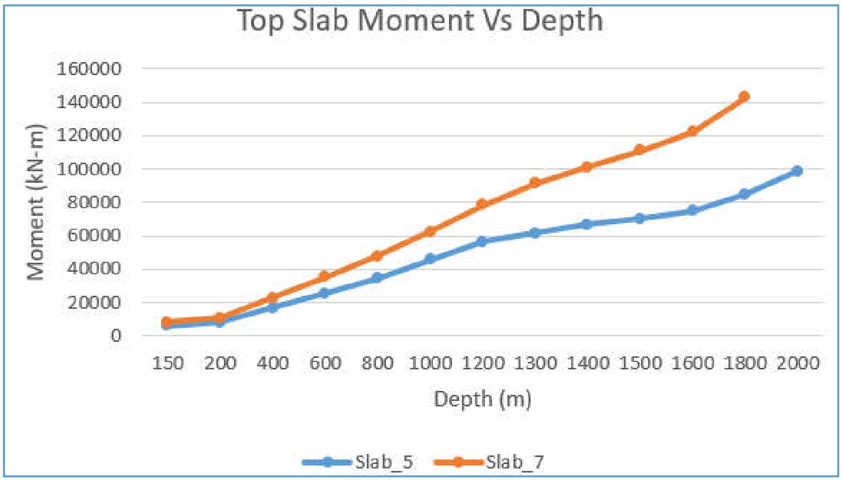

Figure 14 Top Slab Moment Vs Depth

In Figure 14 it can be seen that the moment on the top slab increases as the depth increases. The increase in hydrostatic pressure on top of the slab results into increase in bending stress and thus it results in increase in moment on top of the slab. It is also observed that the increase in moment in slab having 7m height wall is greater than 5m and this is due to fact that the fixed end moment at slab column junction in 7m height wall is greater than 5m wall. For height refer Figure 10.

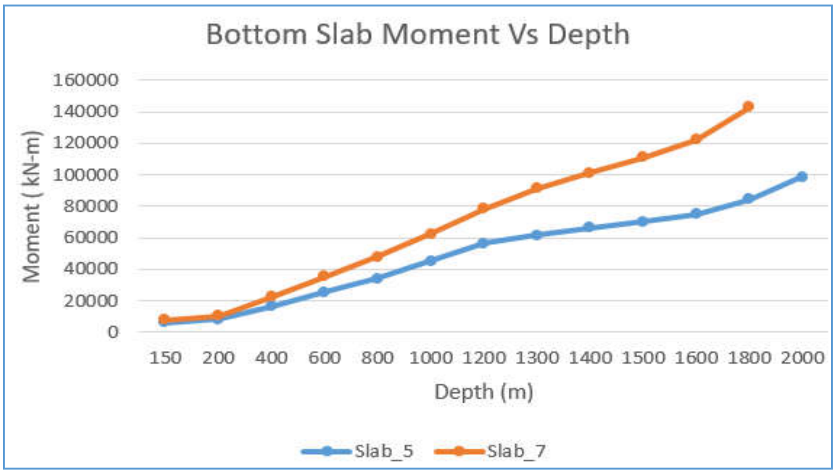

Figure 15 Bottom Slab Moment Vs Depth

In Figure 15 it can be seen that the moment on the bottom slab increases as the depth increases. The increase in hydrostatic pressure on top of the slab results into increase in bearing pressure beneath the bottom slab and thus it results in increase in moment beneath the bottom of the slab. It is also observed that the increase in moment in slab having 7m height wall is greater than 5m and this is due to fact that the fixed end moment at slab column junction in 7m height wall is greater than 5m wall.

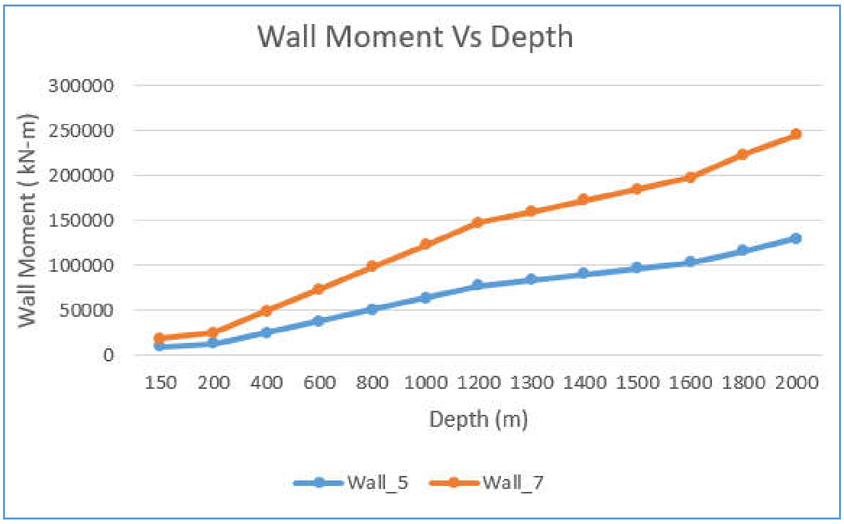

Figure 16 Wall Moment Vs Depth

In Figure 16, with the increase in water depth the fixed end moments at the slab wall junction increases and thus the moment increase for 7 m height wall is more than 5 m height wall.

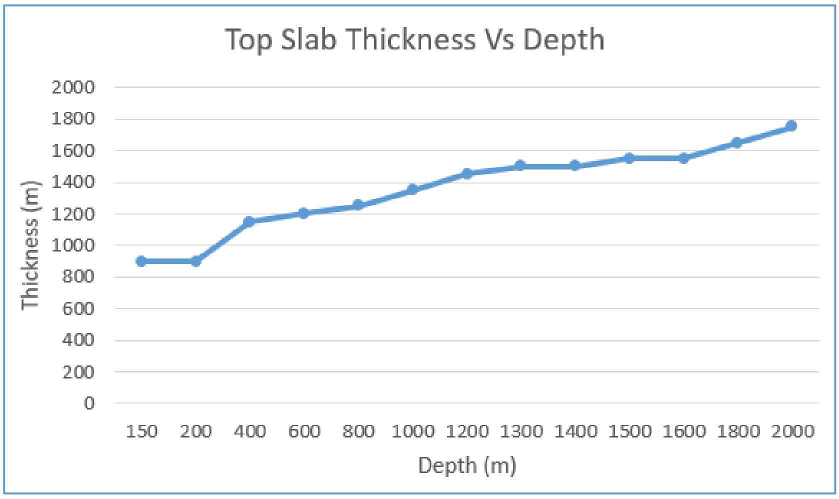

Figure 17 Top Slab Thickness Vs Depth

In Figure 17, it is observed that with the increase in water depth the thickness of slab increases. The increase in hydrostatic pressure on top of the slab results into increase in bending and shear stress and thus it results in increase in thickness of top slab.

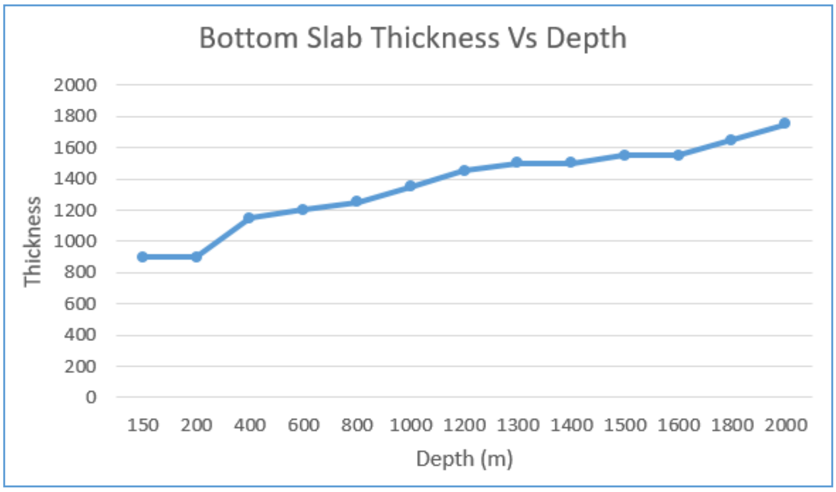

Figure 18 Bottom Slab Thickness Vs Depth

In Figure 18, it is observed that with the increase in water depth the thickness of bottom slab increases. The increase in hydrostatic pressure on top of the slab results into increase in bearing pressure beneath the bottom slab and thus it results in increase in thickness of bottom slab.

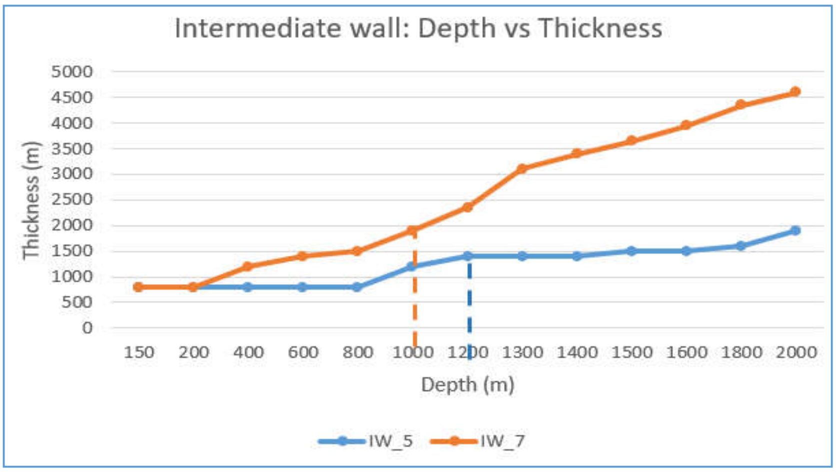

Figure 19 Intermediate wall Thickness Vs Depth

In Figure 19, it can be seen that with the increase in water depth the thickness of intermediate wall increases. As moving down deeper in the water the hydrostatic pressure increases which result in increase of bending stress and shear stress in top slab and which in turn causes increase in the fixed end moment at the slab wall junction.

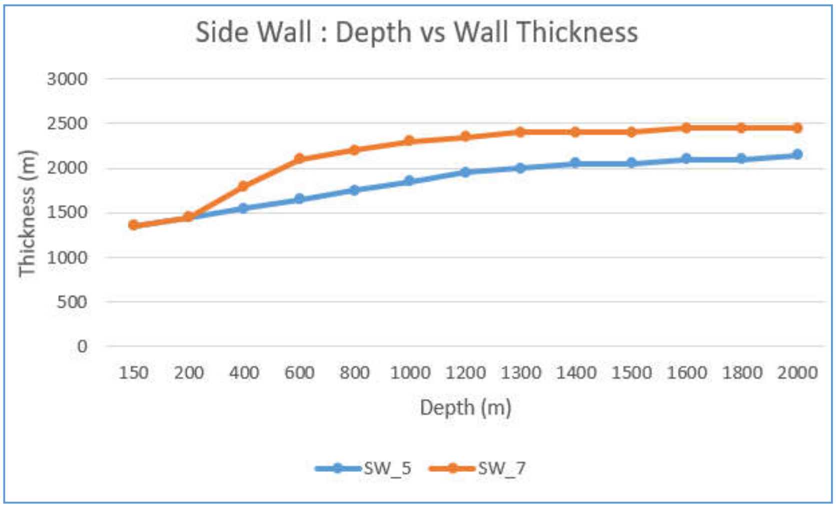

Figure 20 Side wall Thickness Vs Depth

In Figure 20, it can be seen that with the increase in water depth the thickness of side wall increases. As moving down deeper in the water the hydrostatic pressure increases which result in increase of bending stress and shear stress in top slab and which in turn causes increase in the fixed end moment at the slab wall junction.

3.1.6 Discussion

The analysis and design of the subsea storage tank yields the bending moment and shear stress across various cross-section and that in turn helps to obtain thickness of that sections. It is found that as the depth beneath the sea increases there is consequently increase in the bending moment and shear stress. The increase in moment & shear stress causes in increasing magnitude of thickness (slab/wall). The increase in the water depth have impact on the fixed end moments and it increases as the depth increases. The fixed end moment directly results in bending stress on that section. As the water depth increases the hydrostatic pressure increases on the structure and thus fixed end moments increases. The thickness of the wall/slab rely on the fixed-end moments and is generally increases with it. The thickness so obtained are used to fix the configuration of the structure.

3.1.7 Cost

Once the various components of the structure are designed then comes the cost. It is important to see that how cost of the structure varies as the depth increases. As the depth increases the thickness of various cross –section increases and thus the cost of the structure increases. The cost also help to determine which configuration of the structure is economical than the others. It can be observed from Figure 21 that cost of the structure increases as depth increases and the increase in cost for 7m height wall greater than 5m height wall.

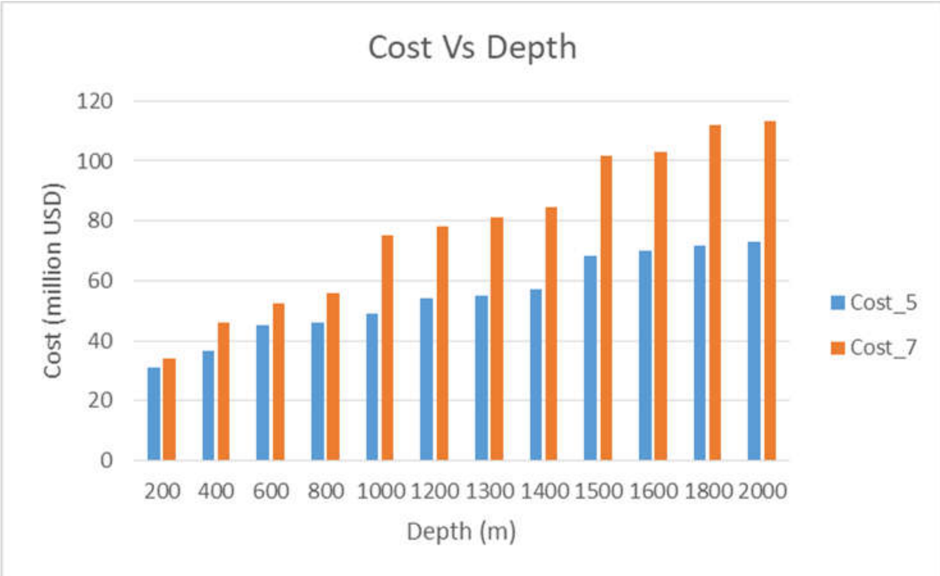

Figure 21 Cost Vs Depth

Cost based on price per unit weight of Concrete/ Reinforcement bar.

Cost of Concrete = (surface area of top slab x thickness of to slab + surface area of bottom slab x thickness of botto slab+ surface area of intermediate wall x thickness of intermediate wall +surface area of side walls x thickness of side wall) (m^3)x cost of concrete($\$/m^3$)

Cost of Reinforcement bars = (length of bars in top slab in longitudinal direction x number of bars x diameter of the bars + length of bars in top slab in transeverse direction x number of bars x diameter of the bars x length of bars in botton slab in longitudinal direction x number of bars x diameter of the bars + length of bars in bottom slab in transeverse direction x number of bars x diameter of the bars + length of bars in walls in longitudinal direction x number of bars x diameter of the bars + length of bars in walls in transeverse direction x number of bars x diameter of the bars + length of bars in sidewalls in longitudinal direction x number of bars x diameter of the bars + length of bars in side walls in transeverse direction x number of bars x diameter of the bars) (m^3) x weight of reinforcement bar(kg/m^3)/ x cost of steel ($/kg)

Total cost of the Structure = Cost of Concrete + Cost of Reiforcement bars
Cost of concrete per meter cube = $ 60 (*Cost Of Concrete Per Cubic Meter | 1m3 Concrete Price | How To Estimate Concrete Cost | Concrete Rate Per Cft | Concrete Rate Per M3*, n.d.)
Cost of reinforcement bar per kg = $ 0.72 (*Check for Current Price of TMT Bars | Scan Steels Ltd.*, n.d.)

3.1.8 Conclusion

To turn Subsea7's conceptual sketch into reality the concrete box is divided into chambers so as to break the length of the top and bottom slab. The holes are provided in the intermediate walls so that water can move from one chamber to another.

As we go into deeper water the hydrostatic pressure increases on the structure and that causes increase in the moment at the center of slab and increase in fixed end moments at the junction of slab and wall. The increase in moment in turn results into the increase in thickness of slab and the wall. Furthermore the fixed end moment develop for 7 m height wall is larger than 5m height wall and thus tank with height 5m is economical than 7m height. There is a factor that limits the depth upto which the tank can be built and that factor is shear stress. As we go deeper into the water the hydrostatic pressure increase and simultaneously shear stress on the structure also increases. It is observed that the shear stress put the limit to 1200m depth for 5m high wall tank and 1000m depth for 7m high wall.

4.0 Selection of pumps and Turbines

4.1 Classifications of turbines

Hydraulic energy is converted into mechanical energy using turbines. Reaction and impulse turbines are the two types of conventional hydro turbines. There is no pressure drop through the moving blades in impulse turbines, whereas the pressure drop is divided between the moving blades and guiding vanes in reaction turbines. The reaction turbines are devices with a low head and a high flow rate. The rotor of a reaction turbine is surrounded by a volute/casing that is completely filled with the running fluid. Turbines come in a number of forms, including axial flow, radial flow, and mixed flow

4.2 Francis turbine: Reaction Turbine

The Francis turbine is designed for medium discharge and head. Francis turbine is a mixed and radial flow hydraulic turbine. It has a tremendous worldwide presence. It is classified as a reaction turbine that uses both hydraulic pressure energy and kinetic energy to operate. It is suitable for head ranges ranging from 20 to 750 meters and power levels ranging from 0.25 to 800 MW per unit (*CHAPTER-3 HYDRAULIC TURBINE CLASSIFICATION AND SELECTION 3.1 Introduction (Reaction Turbines)*, n.d.).
Francis turbines have radial flow, which is confined in a spiral casing that guides water into the runner. To maintain consistent velocity, the casing has a diminishing area as it approaches the row of stationary vanes. Figure 22 depicts a Francis turbine in action.
The energy transfer from the flow to the mechanical energy on the turbine shaft is caused by two effects: To begin, impulse forces are imparted by the change in the directions of the flow velocity vectors via the runner blade channels. This is referred to as the energy conversion's impulse component. Second, it flows from the runner's intake to exit at a drop-in pressure. The reaction portion of the energy conversion is denoted by this symbol.

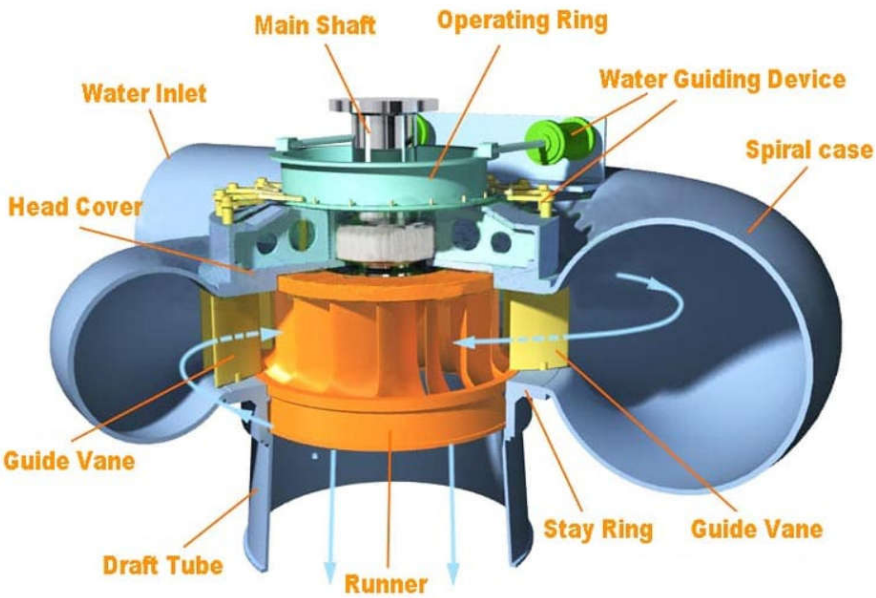

Figure 22 Francis Turbine (Image taken from (Fasi Ur Rahman, 2020)

4.3 Pelton turbine: Impulse Turbine

It is classified as an impulse turbine since there is no pressure drop through the buckets. It has a high head and low discharge with low specific speeds. In a Pelton turbine, the water is accelerated in the nozzle, and the head is converted to velocity, allowing the water to be released at a high rate in the form of a jet. As seen in Figure 23, the jet impacted the buckets attached to the runner's rim. The height of the head varies between 15 and 1800 meters. Its per-unit power varies from 0.5 to 200 MW.

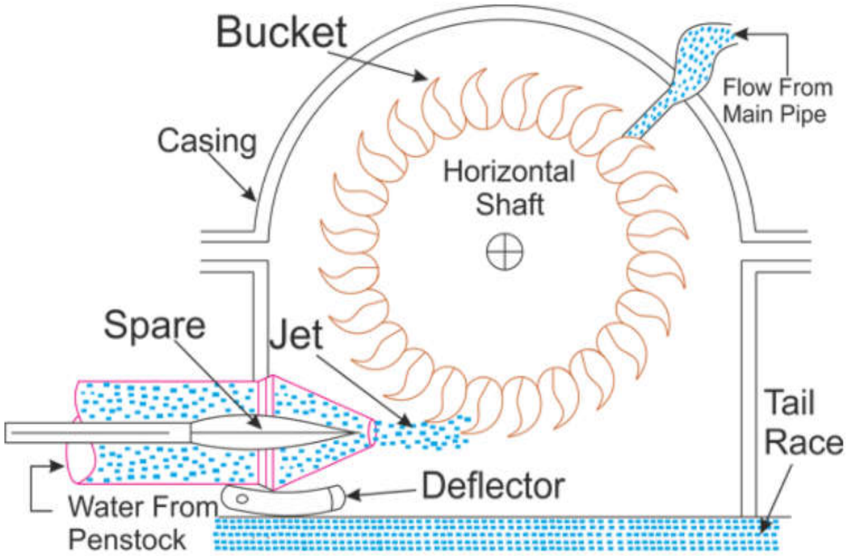

Figure 23 Pelton Turbine
Image taken from (*Pelton Turbine or Pelton Wheel Turbine | MechanicalTutorial*, n.d.)

4.4 Kaplan turbine: Reaction Turbine

Another form of turbine is the Kaplan reaction turbine Figure 24, which operates at low head. In such a turbine, the flow is axial. It is powered by kinetic energy and a little amount of hydraulic pressure energy. With a particular speed of 600-1000, it is ideal for low head and high discharge. Its head spans between 2 and 40 meters, with a power range of roughly 0.1 MW to 120 MW per unit. Both the runner blades and the guide vanes of this turbine are flexible with load, resulting in great efficiency.

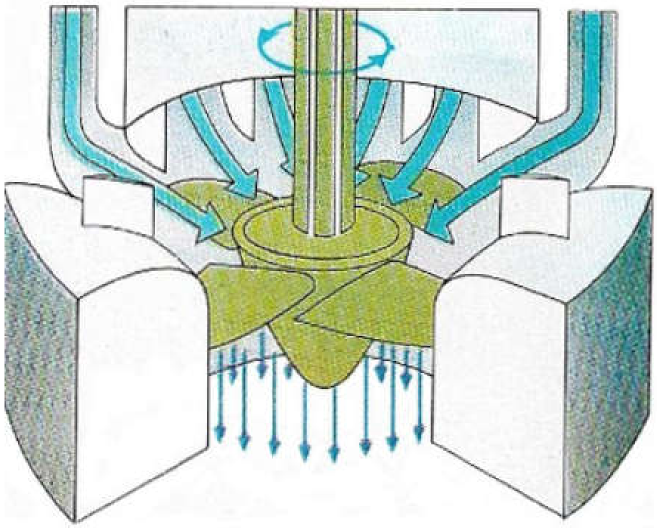

Figure 24 Kaplan Turbine
Image taken from (Suneco, 2017)

4.5 Turbine selection for the case study

Some broad machine prerequisites must be known at the start of the procedure. These would include the necessary head H, rotational speed N, and volumetric flow rate Q for a turbine.

Figure 25 depicts the relationship between the major hydraulic turbines' flow rate Q (m^3/s) and their power capacity P (MW). According to current estimates, a capacity of 550 MW, a Q of 23.8(m^3/s), and a rated head of 1800 m, indicating that Pelton will operate efficiently. Two 300 MW Pelton wheel turbines are required. However, this isn't enough to make a decision as there is another factor that needs to be considered while making the decision and it is specific speed. The particular speed is a non-dimensional quantity. Ns is commonly utilized while deciding on the best machine to use. The value of Ns directs the sort of machine that will meet the design condition's usual demand for high efficiency. Equation 9 is used to compute it.

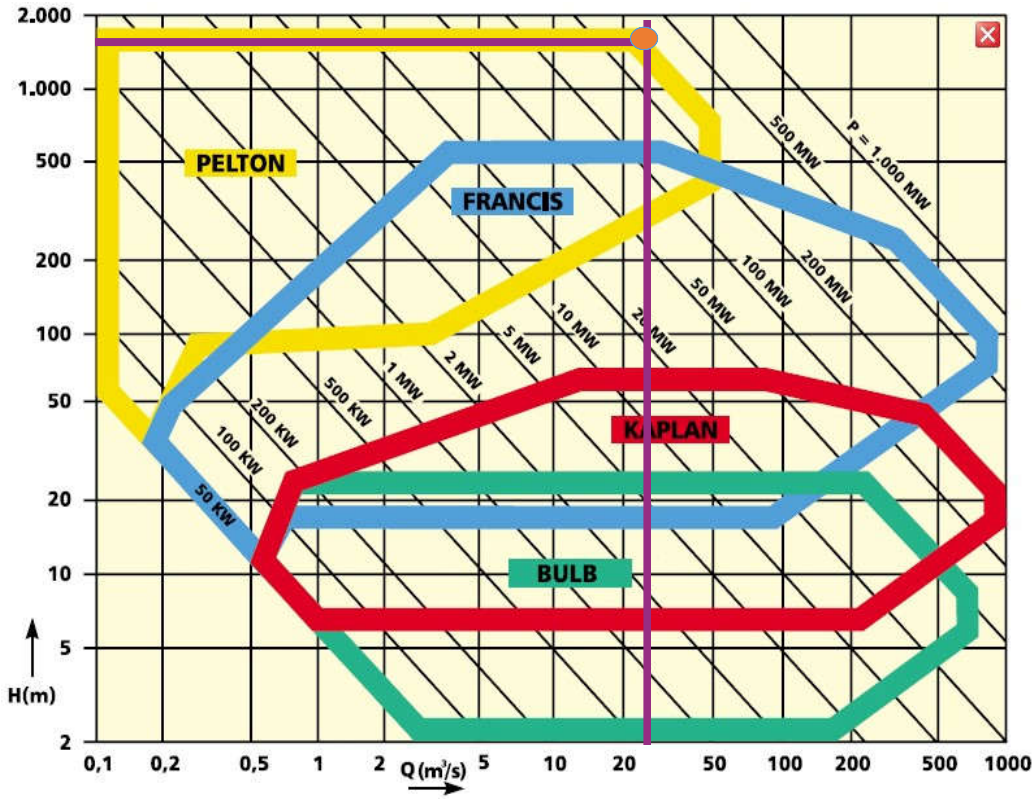

Figure 25 Hydraulic Turbine Selection Chart
Image taken from(S. A. Pereira et al., 2015)

4.6 Specific speed (Ns)

Specific speed is a non-dimensional metric that is frequently used to choose the best machine to employ.

$$Ns = \frac{N \times P^{\frac{1}{2}}}{H^{\frac{5}{4}}} \quad (9)$$

Where: H is the head in m, P the power output in kw, and N_s/N the speed in rev/min of runner.

Table 3 Specific Speed Range (Turbines)

S No.	Ns	Type of Turbine With Best Efficiency
1	8-30	Pelton Wheel with single jet
2	30-51	Pelton Wheel with Multi jet

3	51-255	Francis Turbine
4	255-860	Kaplan Turbine

Table 4 Type of Turbine against available specific speed

Depth	$u = \varphi\sqrt{2gH}$	$N = ux60/(\Pi D)$	$Ns = NP^{1/2}/H^{5/4}$	Turbine
(m)	(m/s)	(rpm)	(rpm)	
200	46,98	498,74	209,69	Francis
400	66,44	705,33	124,69	Francis
600	81,37	863,84	91,99	Francis
800	93,96	997,48	74,14	Francis
1000	105,05	1115,22	62,71	Francis
1200	115,08	1221,66	54,70	Francis

ϕ= The speed ratio varies from 0,6 to 0,9

The ranges of specific speed acceptable for various types of hydraulic turbines are shown in Table 3. The range of Ns for a Francis turbine is described as 51-255. As a result, Francis will be the best turbine for this project for depth 200m to 1200m.

4.7 Pump selection for case study

4.7.1 Diaphragm Pump Positive Displacement Pump

A diaphragm pump Figure 26 is a positive displacement pump that works by a flexible diaphragm moving back and forth in a stationary chamber reciprocating.A membrane or diaphragm separates the pumped fluid from the hydraulic fluid in the pumping chamber. The pulsing action of hydraulic fluid on the driving side causes the diaphragm to flex, causing the volume of the pump chamber to rise and decrease.

The fluid is pushed out via a check valve into a discharge conduit due to a reduction in volume in one chamber causing a rise in pressure in that chamber. In contrast, increasing the volume of one chamber causes the pressure in that chamber to drop, allowing additional fluid to be sucked into the chamber via a check valve. Compressed air, hydraulic oil, steam, or seawater can all be used as hydraulic fluids.

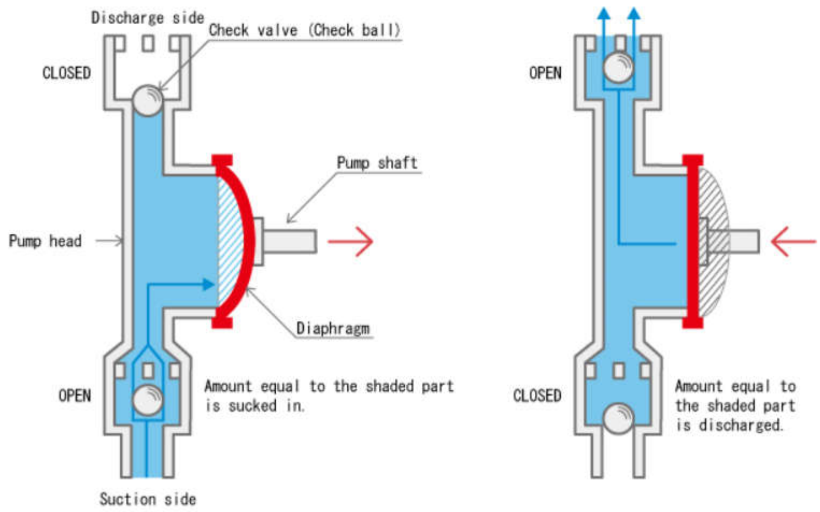

Figure 26 Cross section of Diaphragm Pump
Image taken from (CORPORATION, 2018)

4.7.2 Piston Pump

A piston pump in Figure 27 moves fluid through a cylindrical chamber along an axis by the reciprocating action of a piston rod or plunger. Pressure builds up in the cylinder as the piston passes through it, forcing the fluid to be pushed through the pump. The suction and discharge valves are actuated by the pressure in the cylinder. Due to the to and fro movement of the piston in the cylinder, the fluid flow through the pump pulsates. The primary mover might be steam, a turbine hydraulic drive system, or an electric motor.

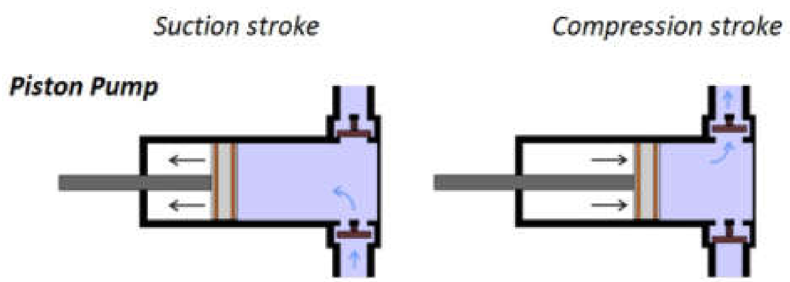

Figure 27 Cross section of Piston Pump
Image taken from **(Smith, 2021)**

4.7.3 Disc Pump

To draw the fluid through the pump, it uses the boundary layer/viscous drag concept. The pump produces a laminar, pulsation-free flow.
The space between successive discs on the earliest disc pumps was extremely tiny. The pump's capacity to handle viscous fluids and particles was severely hampered as a result. The pump's efficiency was likewise

severely restricted. The boundary layer / viscous drag principle may be extended up to 20 inches between consecutive discs while the boundary layer / viscous drag principle remained effective.

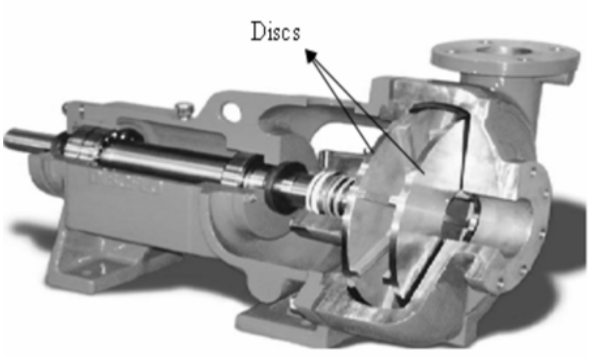

Figure 28 Cross section of Disc Pump
Image taken from (OLUWADAIRO, 2007)

4.7.4 Centrifugal Pump

Centrifugal pumps in Figure 29 work by converting a velocity head to a static head to create pressure. A centrifugal pump has a central revolving wheel or impeller that gives the incoming fluid a high velocity. As the fluid flows past the impellers, centrifugal forces are generated, imparting angular momentum to the fluid and therefore increasing its energy. In the diffusing portion of the pump casing, this energy is transformed into a static pressure head. Centrifugal pumps have quite high rotation rates, ranging from 1500 to 3600 revolutions per minute. However, some high-speed designs have speeds ranging from 5000 to 25000 revolutions per minute.

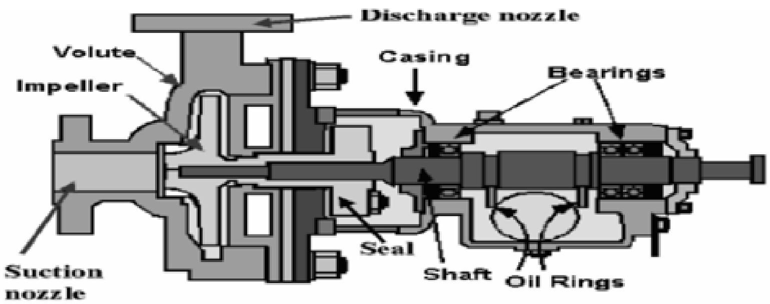

Figure 29 Cross section of Centrifugal Pump
Image taken from (OLUWADAIRO, 2007)

Specific speed of Pump

$$N_S = \frac{N\sqrt{Q_{bep}}}{(H_{bep})^{0.75}} \qquad (10)$$

Where
N_s = Specific speed
N = Rotative speed of the impeller (rev/min)
Q_{bep} = Discharge m^3/s
H_{bep} = Net head developed (m)

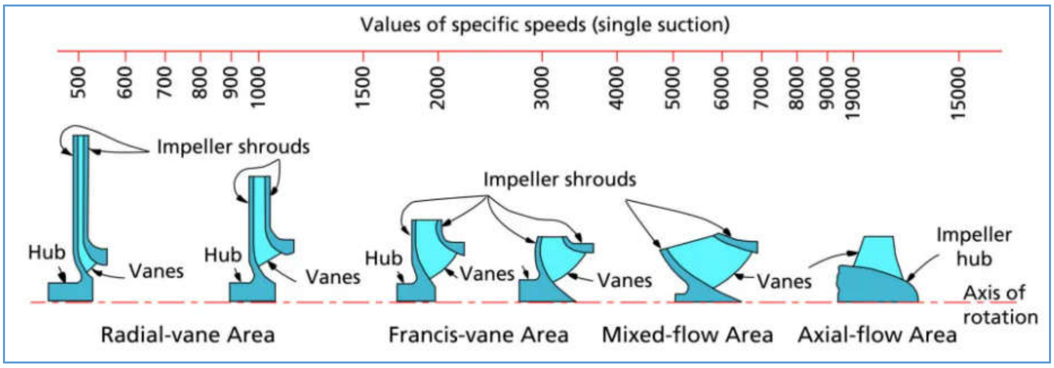

Figure 30 Specific Speed
Image taken from (*Specific Speed (Ns) Definition* | *Intro to Pumps*, n.d.)

4.8 Power Required by Pump

The power required by pump is given by below equation

$P_{h(kW)} = Qx\rho xgxh/1000$ (10a)

Where
ρ (kg/m^3) stands for the density of the fluid to be pumped; water in this case,
g is for acceleration due to gravity (m/s^2) and
H head(m)
Q volumetric flow rate(m^3/s) respectively.

In Present case
ρ = 1000 (kg/m^3)
g = 9,8 (m/s^2)
h = Varies from (100m to 1200m)
Q = 23,5 m^3/s (Assuming the rate of charge is equal to rate of discharge)

After putting values the Power required is 277 MW for 1200 m depth. The most powerful centrifugal pump in the world is Nijhuis HP1-4000.340 which delivers the horse power of 5364 (4MW) with flow rate of 60,000 litres/second (60 m3/second)(*The World's Most Powerful Water Pump - PRESSURE WASHR*, n.d.) . Thus there are 69 pumps of 4 MW required to discharge the tank. Similarly power required for various depths are obtained and is shown in table 5 and based on it required number of pumps are obtained.

Table 5 No. of pumps against depth

Depth	P_h(MW)	No. of Pumps
200	46	12
400	92	23
600	138	35
800	184	46
1000	231	58
1200	277	69

4.9 Comparison of Pump Technologies

Table 6 Comparison of Pump Technologies

		Centrifugal Pump	Disc Pump	Diaphragm Pump	Piston Pump
Pressure	Bar	400	96	448	345
Efficiency	%	30- 85	35-50	85	> 85

Table 6 shows the comparison of various pump technologies (OLUWADAIRO, 2007) and (Parr, 2011) in terms of pressure and efficiency. Since, in our case the max pressure is 120 bar and thus centrifugal pump is selected as it operates at pressure level of 400 bar and can have 85% efficiency.

Tabel 6a Comparison of hydraulic pump types

Type	Maximum pressure (bar)	Maximum flow ($l\ min^{-1}$)	Variable displacement	Positive displacement
Axial piston (swash plate)	350	750	Yes	Yes
Axial piston (valved)	500	1500	Yes	Yes
In-line piston	1000	100	Yes	Yes

Though piston pump can also be selected since it can withstand higher pressure but it cannot deliver a required discharge of 23.8m^3/s. Refer table 6a for the piston pump's flow rate (Parr, 2011).

4.10 Separate VS combined pump/turbines

With a separate pump and turbine:

• Reduces the time it takes to switch between pumping and generation modes.

• Requires extra electrical-mechanical equipment, resulting in higher production expenses.

With a combined pump/turbine:

• More cheap electrical-mechanical equipment and smaller, less costly combinations.

• As a result of the blade having to totally halt and reverse course to changeover modes, the transition between pumping and producing modes takes longer.

4.11 Conclusion

Preliminary selection of the turbine is done by using hydraulic turbine selection chart. The chart shows what type of turbine to be used corresponding to particular head and discharge. So for a head of 1200 m it indicate Pelton turbine as the appropriate turbine. But there is another factor that needs to be considered while making a decision on selection of turbine and that is specific speed. And as per specific speed, Francis turbine is suitable for depth 200m to 1200m. The number of turbines are required as six and each with 75 MW. The rate of charge is considered as rate of discharge and thus there are 12 pumps of 4MW is required for the depth of 200m and the numbers of pumps increases to 69 for the depth of 1200m. The flow rate is 23.8 m^3/s and it can be achieved by using the world's powerful pump that is Nijhuis HP1-4000.340.

5.0 Economic study

5.1 LCOS

The calculation of LCOS for SPHSP includes the capital investment costs, operation and maintenance costs and different discount rates. To calculate the SPHSP's LCOE, the following equation is used:

$$LCOS = \frac{\sum_{t=1}^{n} \frac{I+M+F}{(1+r)^{\wedge} t}}{\sum_{t=1}^{n} \frac{E}{(1+r)^{\wedge} t}} \tag{12}$$

LCOS = the average lifetime levelized cost of Storage in \$/kWh.

I = investment expenditures in the year t.

M= operation and maintenance expenditure in the year t.

F= fuel expenditure in the year t.

E = electricity stored in the year t.

r = discount rate.

n = economic life of the system.

The investment costs are the expenses of constructing SPHSP, which include all capital costs (overnight costs) and the investments necessary to pay them. These funds are mostly used for SPHSP engineering, procurement, and construction, which includes civil, mechanical, and electrical work.

The operations and maintenance (O&M) expenses are separated into fixed O&M costs and backup water costs, and they are needed to guarantee the effective functioning of the SPHSP. These expenses include wages and salary for SPHSP operators and engineers, as well as replacement parts and mechanical and electrical equipment repair. The annual expenses of O&M are sometimes expressed as a percentage of the initial cost per kW. The typical percentage ranges from 1% to 4%. Large hydropower projects generally have a 2 percent to 2.5 percent return on investment. Small hydropower projects do not benefit from economies of scale, and O&M expenses might range from 1% to 6%, or even more in extreme circumstances (Renewable Energy Agency, 2012).

The opportunity cost of capital, or the return on investments lost elsewhere by committing capital to the enterprise under discussion, is the discount rate. In a discounted cash flow (DCF) analysis, it refers to the interest rate used to determine the present value of future cash flows. It is used to account for not just the time value of money, but also the future uncertainties and risks that the cash flow may face; the higher the projected future risks and uncertainties, the higher the discount rate is expected. A discount factor (DF) is the amount by which any future value must be multiplied to turn it into present value, and it can be computed using Eq. (12): where DF is the discount factor; t, the number of periods (years) separating the future and present value; and r, the discount rate.

$$\mathrm{DF} = \frac{1}{(1+r)^t} \tag{12}$$

the values of *r* were assumed to be 8, 10, 12 and 14% (Abdellatif et al., 2018)

Table 7 Lcos Calculation

	Depth (m)	200	400	600	800	1000	1200	
	Items	m$	m$	m$	m$	m$	m$	kWh
CAPEX	Feasibility Study	3	3	3	3	3	3	
	Site Survey	5	5	5	5	5	5	
	R & D expenses	4	4	4	4	4	4	
	Concrete Tank (For 5m High Wall)	30,87	36,77	45,08	46,11	49,13	54,17	
	Pumps	0,53	1,02	1,55	2,03	2,56	3,05	
	Turbines 75 MW (8 No.)*	600	600	600	600	600	600	
Total		643,401	649,787	658,627	660,144	663,694	669,22	
OPEX (1%)	1% of CAPEX	6,43401	6,49787	6,58627	6,60144	6,63694	6,6922	
Electricity Generation								16425000
	LCOS	7,02E+08	7,09E+08	7,18E+08	7,2E+08	7,24E+08	7,3E+08	
		1,61E+08	1,61E+08	1,61E+08	1,61E+08	1,61E+08	1,61E+08	
	LCOS =	4,357	4,400	4,460	4,471	4,495	4,532	
		$/kWh						

In Table 7 feasibility study is considered as 3 and R & D is considered as 4 as mentioned in Aki,2011

*Cost of the turbine is taken from the Figure 31.

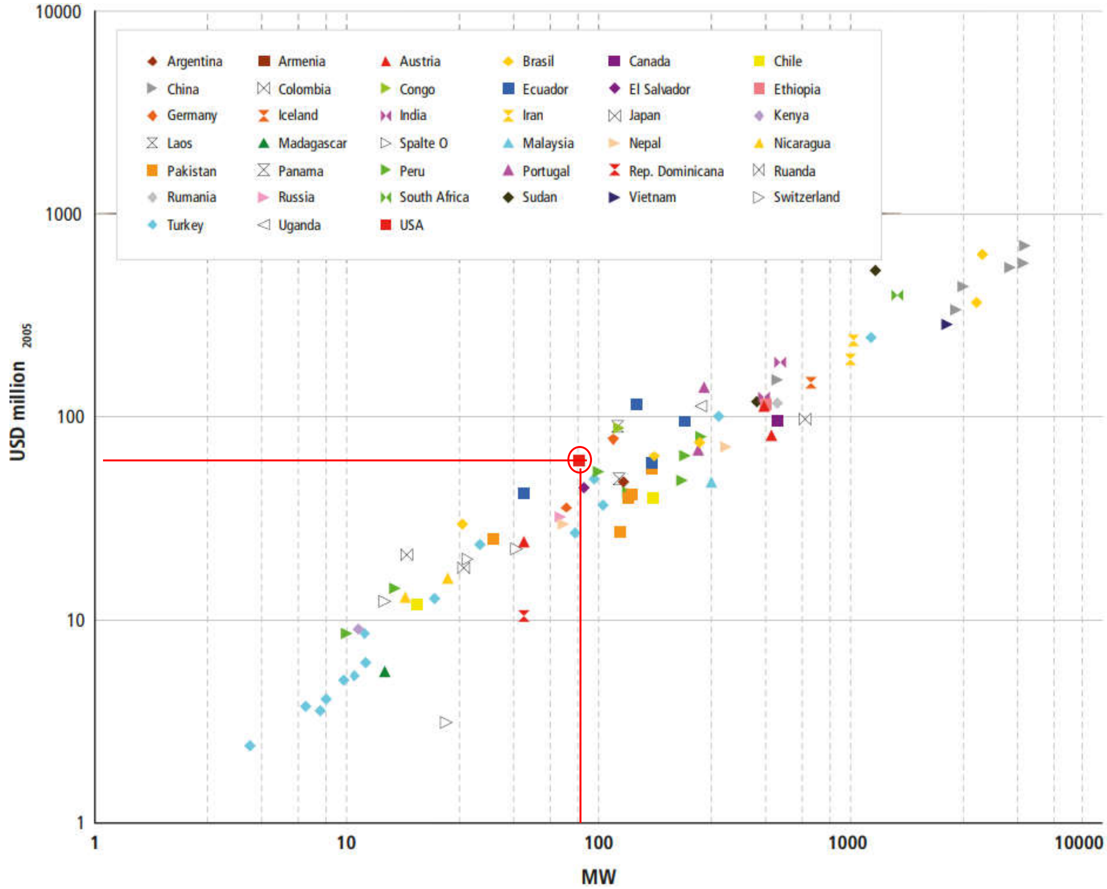

Figure 31 Electro-mechanical equipment for hydro as a function capacity by country (log-scale)

Figure taken from [RE_Technologies_Cost_Analysis-HYDROPOWER]

5.2 Sensitivity Analysis

A sensitivity analysis is conducted in order to assess the influence of different cost parameters. Discount rate varies from 8 % to 14 %. Thus its impact on the LCOS are shown in figures 32 to 35.

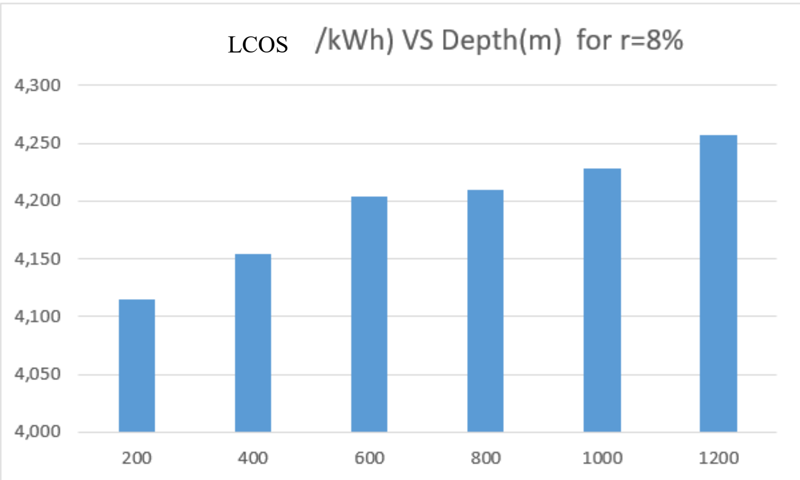

Figure 32 Cost vs Depth with r = 8%

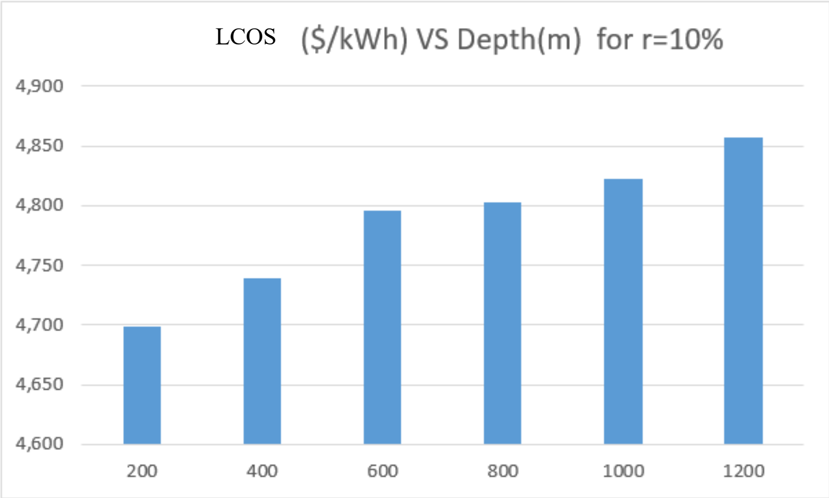

Figure 33 Cost vs Depth with r = 10%

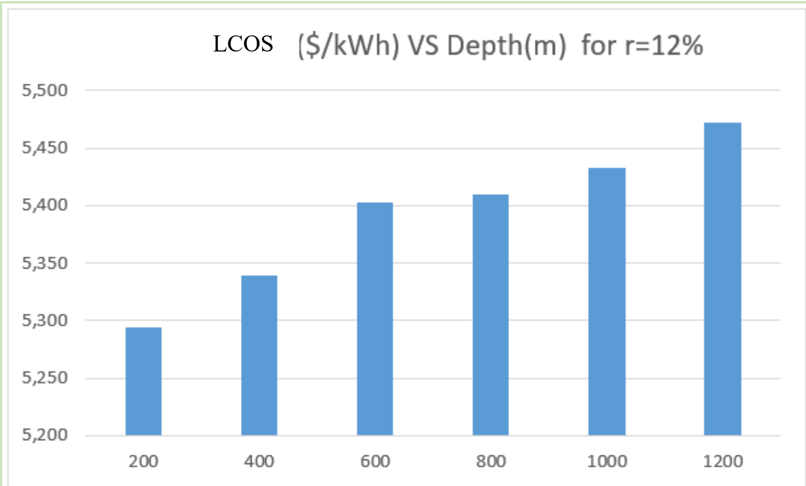

Figure 34 Cost vs Depth with r = 12 %

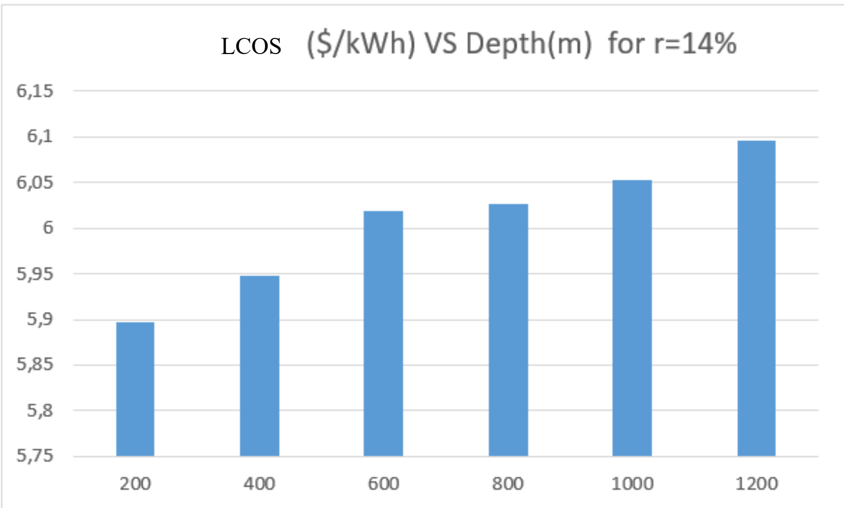

Figure 35 Cost vs Depth with r = 14

The impact of the discount rate over the LCOS is studied and from Figure 32 to 35, it can be concluded that as discount rate increases correspondingly LCOS also increases. The discount rate shows a linear relationship with the LCOS. The higher discount rate makes a SPHSP significantly more expensive in the future.

6.0 Ground Improvement

Because of the tank's design, the earth beneath it may be exceedingly loose and unable to sustain the imposed weights. In other words, huge elastomeric settlements may occur in soil. In this scenario, improving the technical characteristics of in situ-soil is critical.

Currently, a variety of approaches for improving soil are accessible.

Grouting is a ground improvement technique that may be applied to both rock and soil.

It entails injecting liquid ingredients under pressure into a rock or soil in order to alter its engineering characteristics. The grouting procedure can improve the following characteristics:

1. The danger of liquefaction, permeability, and compressibility can all be reduced.
2. It is possible to enhance shear strength.
3. Longevity is a possibility.
4. Swelling and shrinking can be managed.

Grouting can be done in four different ways:

6.1 Chemical (Permeation) Grouting
6.2 Slurry (Intrusion) Grouting
6.3 Jet (Replacement) Grouting
6.4 Compaction (Displacement) Grouting

6.1 Chemical Grouting

Chemical grouting is the process of injecting a chemically permeable, low viscosity substance into sandy soil or rock under low pressure. This technique is commonly used to regulate water flow and produce sandstone-like masses capable of carrying the imposed weights. Because this approach is used at low pressure, the soil's engineering qualities remain unchanged, and only its mechanical properties, such as permeability and porosity, can alter. Figures 36 depict the chemical grouting procedure.

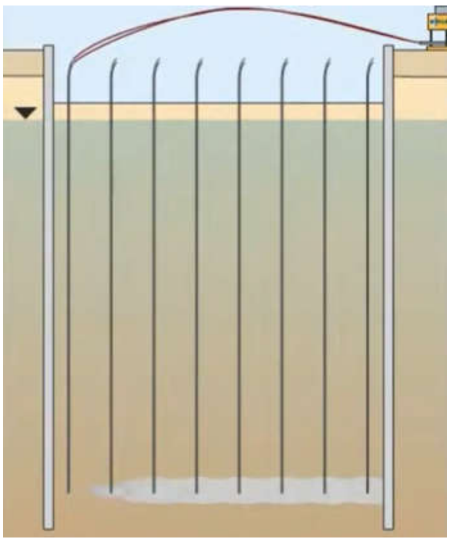

Figure 36 Chemical grouting process

Image taken from (*Permeation (Chemical) Grouting | Keller North America*, n.d.)

6.2 Slurry grouting

Slurry grouting (also known as cement grouting) is the process of injecting a low viscosity, flowable particle grout under high pressure into gaps and fractures in a soil. Because the N (*) (adjusted) levels of most tunnel-route soils are less than 11, this grouting is not practicable. Figure 37 depicts the slurry grouting application method.

$$N = \frac{D15\ (soil)}{D_{85}\ (grout)}$$

Where D is the grain size.

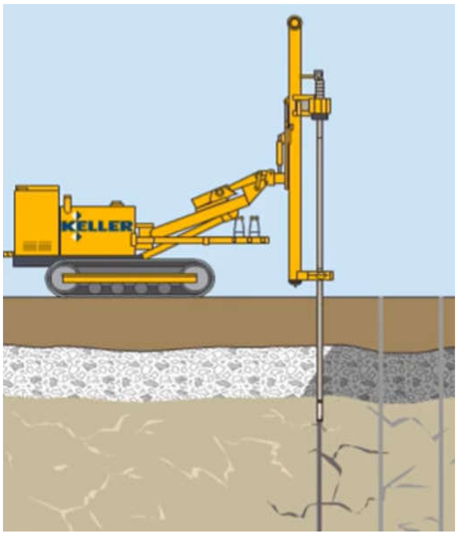

Figure 37 Slurry grouting process

Image taken from (*High Mobility (Cement Slurry) Grouting | Keller North America*, n.d.)

The following are some of the uses for Slurry grouting:

- Rock foundation treatment of a dam site
- Rock cut-off curtains
- Pressure injected anchors
- Stabilization of gravels and shotcreted rock

6.3 Jet Grouting

Jet Grouting is a flexible ground modification method that is used to generate in-situ, cemented soilcrete formations. The injection pipe is put into the soil at a suitable depth to produce soilcrete. The soil is then exposed to a horizontal high-pressure air water jet while also being combined with grout,

which improves the soil's engineering characteristics. The most significant benefit of this technique is that it may be used on any type of soil. Figure 38 depicts the jet grouting procedure.
The following are some of the uses for jet grouting:

- Control of underground fluids
- Excavation of unstable soil
- Increase the bearing capacity of soil

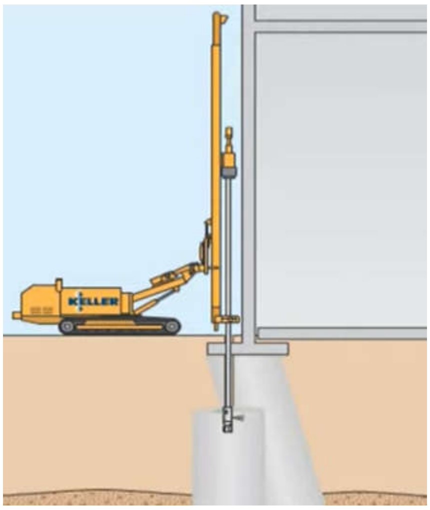

Figure 38 Jet grouting process
Image taken from (*Jet Grouting | Keller North America*, n.d.)

6.4 Compaction Grouting

Compaction Grouting is the process of injecting a viscous (low-mobility) aggregate grout under high pressure into the surrounding soil to displace and compress it. This technique may be used in any type of soil and even underwater, however it works best in soils that are finer than medium sands. One of the most significant benefits is that it has the greatest impact in the poorest soil zones. The compaction grouting process is shown in Figure 39.

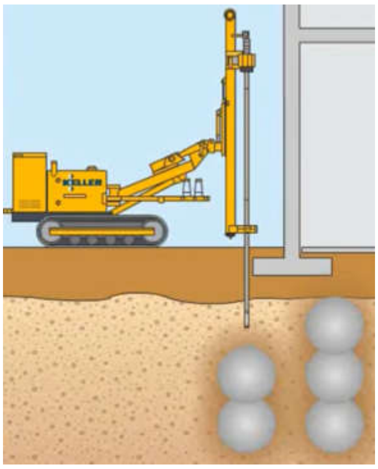

Figure 39 Compaction Grouting Process
Image taken from (*Low Mobility (Compaction) Grouting | Keller North America*, n.d.)

Compaction grouting applications:

- Soil densification prior to building
- Prevention of settlement in tunneling through soft ground
- Provide underpinning for structures
- Strengthen the supporting ground
- Increase the bearing capacity of the founding soils Subsoil liquefaction danger is being reduced.

6.5 Encountered Soil Issues

The seabed might be made up of fine to coarse silty sands/sandy silts with low SPT-N penetration values. The soil has the consistency of a deep marsh, with penetration values of less than 2. As a result, the soil's bearing capacity is insufficient to withstand the stresses transmitted to it, resulting in extremely massive and unpleasant total and differential settlements beneath the tank foundation. As a result, a ground improvement procedure must be implemented at the tunnel alignment site. The reasons to make ground improvement are;

- Increasing bearing capacity
- Strengthening the ground's shear strength
- Reducing the danger of liquefaction
- Reducing unacceptable settling

6.5.1 Which Method should be used?

Because it is the most appropriate technique for treating the problems of the seabed soil, the chosen method for loose soil is the ‘compaction grouting' type ground renovation method. When four techniques are compared, the justification for choosing this method is as follows:

Chemical grouting addresses the soil's mechanical qualities, such as permeability and porosity, but because it is applied at low pressure, it has no influence on the soil's engineering properties. However, grouting is required to enhance the tank seabed's shear strength and settlement characteristics, as total settlements of more than 2.5 cm cannot be permitted beneath the tank.

The slurry technique is acceptable for rocks and gravels with N levels greater than 11, but not for loose soils, despite the fact that it is administered under high pressure. Jet grouting is not an injection procedure, but rather a sort of mixing technique that may be utilized for most soil types. Jet grouting is mostly used to avoid excessive settlement beneath column foundations or to create an impermeable barrier to water leaks in tunnels. Furthermore, whether this approach reduces the soil's liquefaction risk is still a point of contention. Furthermore, the procedures described above are not suitable for use underwater. However, because it is a displacement technique, compaction grouting is especially useful for vast areas, such as undersea constructions, because it compacts the soil by displacing it. Because this approach causes more compaction of the surrounding soil, the soil's engineering characteristics improve as well. Furthermore, it is suggested for liquefiable soils to mitigate this disadvantage.

As a result, when all of the ground improvement approaches are weighed, compaction grouting emerges as the best option for meeting the demands of the seabed soils along the tank route. Furthermore, research reveals that compaction grouting is the most often used enhancement method for submerged tank. When compaction grouting type ground improvement is used, the seabed soil area to be treated should be 5 m greater on both sides of the tank base. Due to the stress bulb extension at depth beneath the tank foundation level, (i.e. Width+2*5). This also aids in reducing future bearing capacity/shear failure issues at the tank base's margins.

6.6 Conclusion

In order to increase the bearing capacity of the soil and reduce the liquefaction risk, ground improvement was recommended and it was determined that the most appropriate improvement type is compaction grouting, since this method provides the opportunity to change the engineering properties of the seabed soil.

7.0 Constructability

This pictures below shows one of the method on how the immersed tank will be built and installed.

The all of the immersed tank elements will be produced in a workshop as shown in Figure 40. The workshops facilities include production halls, docks and a working harbour. The halls where the reinforcing modules will be prepared.

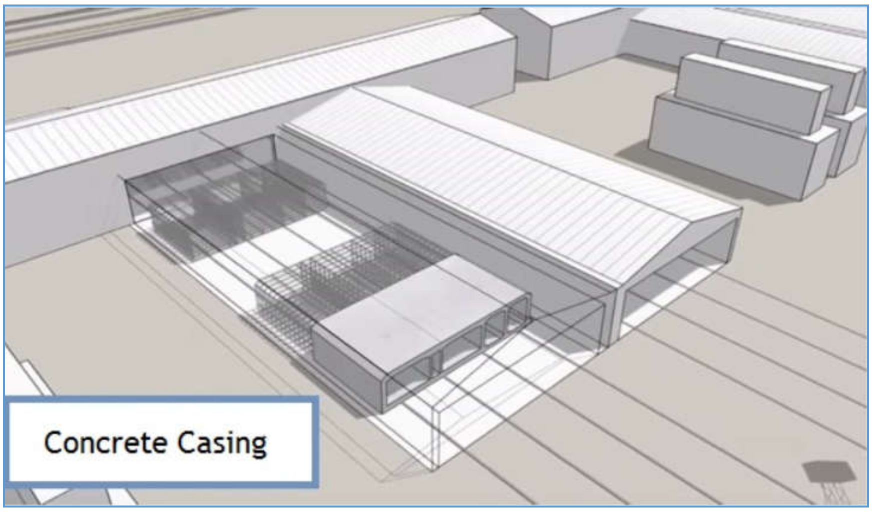

Figure 40 Concrete Casing.
Image taken from (*Immersed Tube Tunnel Analysis*, 2000)

The workshop have several production lines for casting the concrete elements. The Production will take place in an incessant method and in which identical elements are joined to create a complete segment. The finished tank segments is then pushed in the drydock and then prepared for transport. Each element can be 225 metres long. Watertight bulkheads are installed to preparation for shipment, and the drydock is filled with water until the element floats.

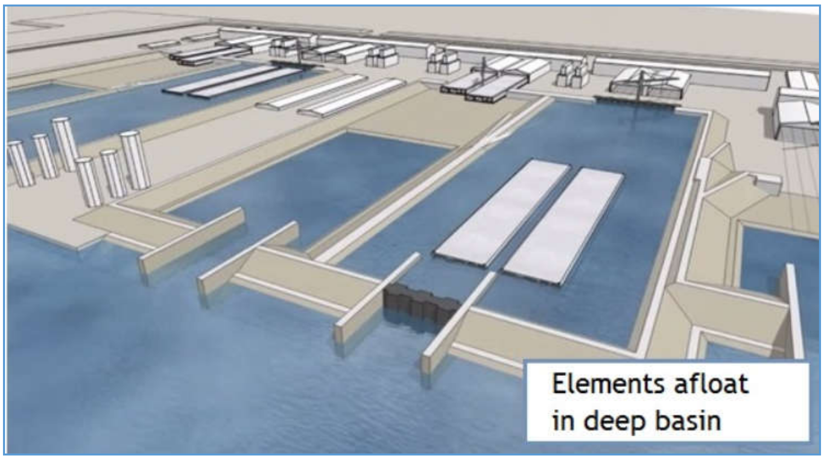

Figure 41 Elements afloat in deep basin
Image taken from (*Immersed Tube Tunnel Analysis*, 2000)

The dock gates are closed after that, and seawater is poured into the basin as shown in Figure 41. Now the floating tank element will be towed to the deep section of the basin. The basin's water level is then reduced to match the harbor's level. The dock gates are thrown open, allowing the element to be towed away as shown in Figure 42. The element is dragged to a holding area near where it will be submerged.

Figure 42 Transport
Image taken from (*Immersed Tube Tunnel Analysis*, 2000)

The element will then be immersed in a trench that was dug ahead of time while the element was being built.

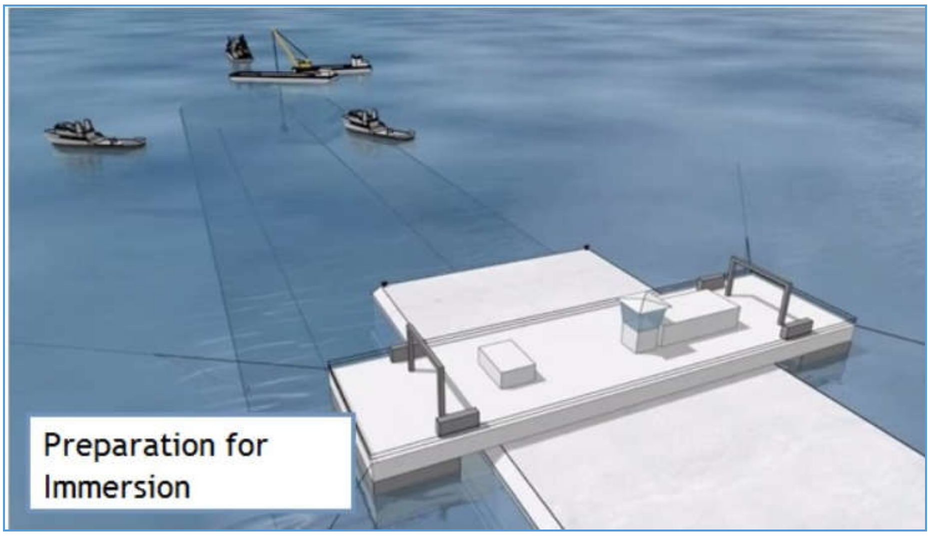

Figure 43 Preparation for immersion
Image taken from (*Immersed Tube Tunnel Analysis*, 2000)

Dredging in the tank trench will be done by specialist dredges to provide a precise and smooth base. Dredging procedures were used to minimize sediment discharge and reduce the impact on the environment and surrounds. The dredged debris will be carried down the coast on barges to approved dump sites.

The tank element will be connected to floating pontoons in the holding area near the trench before being transported to its immersion point as shown in Figure 43. When the element is exactly above the region in which it will be submerged. Cables linked to temporary anchors in the seafloor will keep it in place. The tank portion is now ready to be dropped onto a previously prepared gravel bed base previously been laid in the tank trench as shown in Figure 44.

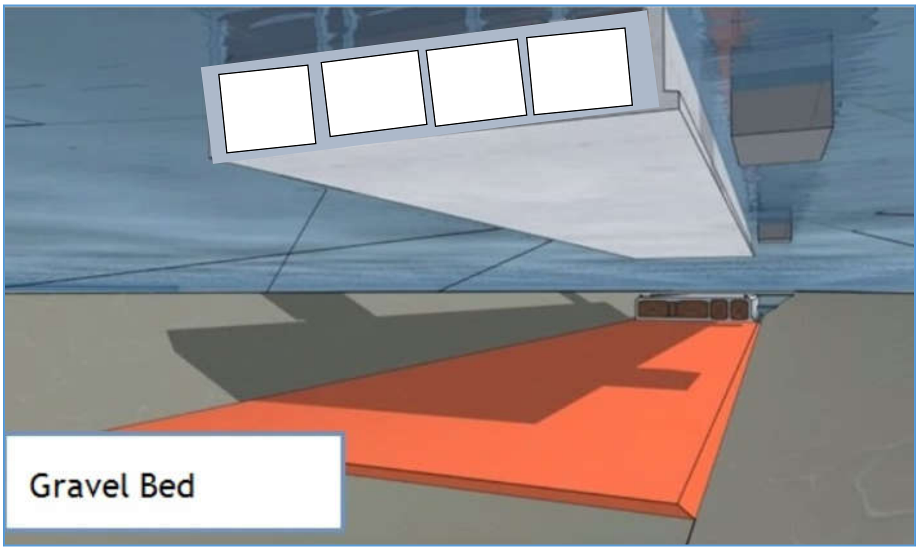

Figure 44 Gravel Bed
Image taken from (*Immersed Tube Tunnel Analysis*, 2000)

The element's ballast tanks are progressively filled with water in order to sink it as shown in Figure 45.

Figure 45 Immersion
Image taken from (*Immersed Tube Tunnel Analysis*, 2000)

The movement of the element is controlled by mooring wires as it lowers slowly. The previous element is linked to the new terminal element. Following that, water is pumped between the bulkheads, and the water pressure on the opposite free end of the element forces the elements closer together, resulting in a watertight seal.

8.0 Conclusion

The influence of SPHSP inclusion in the power system, as well as the rising level of wind power integration in India, was investigated in this study. The following three major features of energy storage system design have been assessed: sizing and the preliminary design of the subsea storage tank, suitable selection of pump and turbines and simplified economic analysis regarding the levelised cost of storage. This study has concluded the following issues:

First one is related with the design and it comes out that with the increase of water depth the moments on structure as well their thickness increases. And it is also observed that there is large increase of bending for 7 m high wall as compared with 5m height wall and thus the tank with the 5m high wall is economical than tank having 7m high wall.

With the increase of the water depth there is tremendous increase of hydrostatic pressure on the structure and this result into large increase of shear stress on the structure. The shear stress is the design driver that limits the depth of Subsea pumped Hydro storage plant tank to 1200 m beneath the sea level.

Since the SPHSP is to be built at the depth of 1200 m beneath the sea level and thus the pumps needs to be chosen in such a way that can bear such hydrostatic pressure. In the current case there are two possibilities that either centrifugal pump to be selected or the piston pump as both can sustain high pressure. Though the piston pump has at the same time has higher efficiency as compared to centrifugal pump but it cannot deliver the required discharge of 23.8 m^3/s and thus centrifugal pump is an ideal selection for the current case. On the other hand, turbine selection is based on specific speed and it comes out that Francis turbine is suitable for depth 200m to 1200m. The levelised cost of storage (LCOS) is also calculated, and it works out to be \$4.53 per kilowatt hour for 1200m depth

9.0 Recommendations

This thesis performed a preliminary Feasibility analysis of Subsea pumped hydro storage plant. The feasibility analysis mainly consist of design of the tank and the economics evaluation of SPHSP. For to carry future work many areas are still need to be touched upon.

Firstly, the tank is designed with the proposed concept from Subsea7 as a wedge shape like structure. With such a configuration the tank can be built up to 1200 m beneath the sea level. If in future we try with different configuration than it may be possible that we can go to larger depth. Other possible structure can be in the form of arch like structure. Secondly, since the structure is going to be built 1200 m below the mean sea level and thus it may require to be analyzed for seismic effect. Furthermore, tank structure is designed as a reinforced cement concrete structure and there are other options that can be look upon such as considering the composite section that is combining steel section with the concrete. With such a design it is possible that shear strength of concrete will increase and thus tank can be built to the larger depth.

Thirdly the structure is analyzed with moment distribution method, so the work can be carried by analyzing the structure with Finite Element Analysis by using special software's such STAAD/ANSYS etc.

10 References

Global pumped storage hydropower capacity 2020 | Statista. (n.d.). Retrieved October 12, 2021, from https://www.statista.com/statistics/689667/pumped-storage-hydropower-capacity-worldwide-by-country/

Abdellatif, D., AbdelHady, R., Ibrahim, A. M., & El-Zahab, E. A. (2018). Conditions for economic competitiveness of pumped storage hydroelectric power plants in Egypt. *Renewables: Wind, Water, and Solar*, *5*(1), 1–14. https://doi.org/10.1186/s40807-018-0048-1

Aki, H. (2011). Energy storage research and development activities in Japan. *IEEE Power and Energy Society General Meeting*. https://doi.org/10.1109/PES.2011.6039460

Anuta, O. H., Taylor, P., Jones, D., McEntee, T., & Wade, N. (2014). An international review of the implications of regulatory and electricity market structures on the emergence of grid scale electricity storage. In *Renewable and Sustainable Energy Reviews* (Vol. 38). https://doi.org/10.1016/j.rser.2014.06.006

ARUP. (2020). *Consortium assessing pumped hydro storage plant in South Australia*. News and Events. https://www.arup.com/news-and-events/consortium-assessing-pumped-hydro-storage-plant-in-south-australia

Barbour, E., Wilson, I. A. G., Radcliffe, J., Ding, Y., & Li, Y. (2016a). A review of pumped hydro energy storage development in significant international electricity markets. In *Renewable and Sustainable Energy Reviews* (Vol. 61). https://doi.org/10.1016/j.rser.2016.04.019

Barbour, E., Wilson, I. A. G., Radcliffe, J., Ding, Y., & Li, Y. (2016b). A review of pumped hydro energy storage development in significant international electricity markets. In *Renewable and Sustainable Energy Reviews* (Vol. 61, pp. 421–432). https://doi.org/10.1016/j.rser.2016.04.019

Barbour, E., Wilson, I. A. G., Radcliffe, J., Ding, Y., & Li, Y. (2016c). A review of pumped hydro energy storage development in significant international electricity markets. *Renewable and Sustainable Energy Reviews*, *61*, 421–432. https://doi.org/10.1016/J.RSER.2016.04.019

Beaudin, M., Zareipour, H., Schellenberglabe, A., & Rosehart, W. (2010). Energy storage for mitigating the variability of renewable electricity sources: An updated review. In *Energy for Sustainable Development* (Vol. 14, Issue 4). https://doi.org/10.1016/j.esd.2010.09.007

Buckley, T., Gupta, A., Garg, V., & Shah, K. (2019). *Flexing India's Energy System Making the Case for the Right Price Signals Through Time-Of-Day Pricing*.

Carolin Mabel, M., & Fernandez, E. (2008). Analysis of wind power generation and prediction using ANN: A case study. *Renewable Energy*, *33*(5), 986–992. https://doi.org/10.1016/j.renene.2007.06.013

CHAPTER-3 HYDRAULIC TURBINE CLASSIFICATION AND SELECTION 3.1 Introduction (Reaction Turbines). (n.d.).

Check for current price of TMT bars | Scan Steels Ltd. (n.d.). Retrieved September 14, 2021, from https://scansteels.com/products-services/product-pricing/

Cochran, J., Bird, L., Heeter, J., & Arent, D. J. (2012). Integrating Variable Renewable Energy in Electric Power Markets: Best Practices from International Experience, Summary for Policymakers. *Nreltp-6a20-60451*, *April*.

CORPORATION, T. (2018). *1-1. Diaphragm Pump: What Is a Diaphragm Pump? | Basics | Learn | TACMINA CORPORATION*. https://www.tacmina.com/learn/basics/01.html

Cost Of Concrete Per Cubic Meter | 1m3 Concrete Price | How To Estimate Concrete Cost | Concrete Rate Per Cft | Concrete Rate Per M3. (n.d.). Retrieved September 14, 2021, from https://civiconcepts.com/blog/cost-of-concrete-per-cubic-meter

Deane, J. P., Ó Gallachóir, B. P., & McKeogh, E. J. (2010). Techno-economic review of existing and new pumped hydro energy storage plant. In *Renewable and Sustainable Energy Reviews* (Vol. 14, Issue 4). https://doi.org/10.1016/j.rser.2009.11.015

Denholm, P., Ela, E., Kirby, B., Milligan, M., Denholm, P., Ela, E., Kirby, B., & Milligan, M. (2010). The Role of Energy Storage with Renewable Electricity Generation The Role of Energy Storage with Renewable Electricity Generation. *National Renewable Energy Laboratory*, *January*.

Storing energy at sea, Forschung-Energiespeicher.Info 4 (2016). http://forschung-

energiespeicher.info/en/projektschau/gesamtliste/projekt-einzelansicht/95/Kugelpumpspeicher_unter_Wasser/
Falk, J. (2013). *Subsea Pumped Hydro Storage*. 1–18. https://www.google.com/search?q=Subsea+Pumped+Hydro+Storage&oq=Subsea+Pumped+Hydro+Storage&aqs=chrome..69i57j0i22i30j69i61.1403j0j4&sourceid=chrome&ie=UTF-8
Fasi Ur Rahman. (2020). *Francis Turbine - its Components, Working and Application*. Theconstructor.Org. https://theconstructor.org/practical-guide/francis-turbines-components-application/2900/
Gross, R., Heptonstall, P., Leach, M., Anderson, D., Green, T., & Skea, J. (2007). Renewables and the grid: understanding intermittency. *Proceedings of the Institution of Civil Engineers - Energy*, *160*(1). https://doi.org/10.1680/ener.2007.160.1.31
Gustafsson, M. (2013). *Degree project in Improved Governing of Kaplan Turbine Hydropower Plants Operating Island Grids*.
High mobility (cement slurry) grouting | Keller North America. (n.d.). Retrieved August 22, 2021, from https://www.keller-na.com/expertise/techniques/high-mobility-grouting
How can we make floating wind farms cost-effective? | World Economic Forum. (n.d.). Retrieved November 3, 2021, from https://www.weforum.org/agenda/2020/07/floating-wind-farms-green-energy-electricity-offshore
Immersed Tube Tunnel Analysis. (2000). http://www.railsystem.net/immersed-tube-tunnel/
Infield, D., & Hill, J. (2014). *Literature Review: Electrical Energy Storage for Scotland*. https://strathprints.strath.ac.uk/57397/
IRENA. (2017). Renewable Energy Prospects for India: A working paper based on REmap. *International Renewable Energy Agency (IRENA)*, *October*. http://www.irena.org/DocumentDownloads/Publications/IRENA_REmap_India_paper_2017.pdf%0ARenewable Energy Prospects for Ukraine
Jet grouting | Keller North America. (n.d.). Retrieved August 22, 2021, from https://www.keller-na.com/expertise/techniques/jet-grouting
Low mobility (compaction) grouting | Keller North America. (n.d.). Retrieved August 22, 2021, from https://www.keller-na.com/expertise/techniques/low-mobility-grouting
Muppandal (India) - Wind farms - Online access - The Wind Power. (n.d.). Retrieved September 19, 2021, from https://www.thewindpower.net/windfarm_en_449_muppandal.php
of Indian Standards, B. (n.d.). *IS 456 (2000): Plain and Reinforced Concrete - Code of Practice*.
Offshore Wind | Ministry of New and Renewable Energy, Government of India. (2021). https://mnre.gov.in/wind/offshore-wind
OLUWADAIRO, T. (2007). AN EVALUATION OF SUBSEA PUMP TECHNOLOGIES THAT CAN BE USED TO ACHIEVE DUAL GRADIENT DRILLING. *Undefined*, *December*.
Parr, A. (2011). Hydraulic Pumps and Pressure Regulation. In *Hydraulics and Pneumatics* (pp. 31–49). Elsevier. https://doi.org/10.1016/b978-0-08-096674-8.00002-1
Pazheri, F. R., Othman, M. F., & Malik, N. H. (2014). A review on global renewable electricity scenario. In *Renewable and Sustainable Energy Reviews* (Vol. 31, pp. 835–845). https://doi.org/10.1016/j.rser.2013.12.020
Pelton Turbine or Pelton Wheel Turbine | MechanicalTutorial. (n.d.). Retrieved August 22, 2021, from https://www.mechanicaltutorial.com/pelton-turbine-or-pelton-wheel-turbine
Permeation (chemical) grouting | Keller North America. (n.d.). Retrieved August 22, 2021, from https://www.keller-na.com/expertise/techniques/permeation-chemical-grouting
Power Technology. (2020). *What are the most used renewable energy sources in the world?* Power Technology. https://www.power-technology.com/features/featurethe-worlds-most-used-renewable-power-sources-4160168/
S. A. Pereira, B., Sobrinho, P., & Silveira, J. (2015). *The use of LINGO programming language to develop a computer tool to provide a technical and economic analysis of a hydraulic potential that allows the application of Francis turbines and Kaplan turbines*. *May 2016*, 98–99. https://www.researchgate.net/publication/302969536_The_use_of_LINGO_programming_language_to

_develop_a_computer_tool_to_provide_a_technical_and_economic_analysis_of_a_hydraulic_potential_that_allows_the_application_of_Francis_turbines_and_Kaplan_turbin

Sant, A., & Thakare, N. (2019). Enabling Fast Response Ancillary Services Using Pumped Storage Hydro Power Projects. *2nd Int'l Conference on Large-Scale Grid Integration of Renewable Energy in India*, 1–8. https://regridintegrationindia.org/wp-content/uploads/sites/14/2019/11/7A_5_RE_India19_051_presentation_ANANT_SANT.pdf

Sivakumar, N., Das, D., Padhy, N. P., Senthil Kumar, A. R., & Bisoyi, N. (2013). Status of pumped hydro-storage schemes and its future in India. In *Renewable and Sustainable Energy Reviews* (Vol. 19). https://doi.org/10.1016/j.rser.2012.11.001

Smith, R. (2021). *Useful information on positive displacement pumps.* Pump Specialist UK - Michael Smith Engineers. https://www.michael-smith-engineers.co.uk/resources/useful-info/positive-displacement-pumps

Specific Speed (Ns) Definition | Intro to Pumps. (n.d.). Retrieved August 22, 2021, from https://www.introtopumps.com/pump-terms/ns-specific-speed/

Suneco. (2017). *Kaplan Turbine Generator*. 10. https://www.daviddarling.info/encyclopedia/K/AE_Kaplan_turbine.html

TANGEDCO. (2017). *Tamil Nadu Generation and Distribution Corporation Limited (TANGEDCO)*. GoTN. https://www.tangedco.gov.in/

Thapar, O. D. (2015). HYDRAULIC TURBINE CLASSIFICATION AND SELECTION 3.1 Introduction (Reaction Turbines). *Modern Hydroelectric Engineering Practice*, 53–109.

The World's Most Powerful Water Pump - PRESSURE WASHR. (n.d.). Retrieved October 29, 2021, from https://pressurewashr.com/the-worlds-most-powerful-water-pump/

Top 10 countries in wind energy capacity | REVE News of the wind sector in Spain and in the world. (n.d.). Retrieved September 30, 2021, from https://www.evwind.es/2021/05/24/top-10-countries-in-wind-energy-capacity/80896

United State Environmental Protection Agency. (2018). Sources of Greenhouse Gas Emissions | Greenhouse Gas (GHG) Emissions | US EPA. In *Greenhouse Gas Emissions*. https://www.epa.gov/ghgemissions/sources-greenhouse-gas-emissions

Wind Resources in India. (n.d.). Retrieved August 22, 2021, from https://www.mapsofindia.com/maps/nonconventional/windresources.htm

Yang, C. J., & Jackson, R. B. (2011). Opportunities and barriers to pumped-hydro energy storage in the United States. In *Renewable and Sustainable Energy Reviews* (Vol. 15, Issue 1). https://doi.org/10.1016/j.rser.2010.09.020

Zeng, M., Zhang, K., & Liu, D. (2013). Overall review of pumped-hydro energy storage in China: Status quo, operation mechanism and policy barriers. In *Renewable and Sustainable Energy Reviews* (Vol. 17). https://doi.org/10.1016/j.rser.2012.05.024

Zhu, B. S., & Ma, Z. (2019). Development and Prospect of the Pumped Hydro Energy Stations in China. *Journal of Physics: Conference Series*, *1369*(1), 12018. https://doi.org/10.1088/1742-6596/1369/1/012018

11 Appendices

Appendix 1: Volume calculation of Subsea Pump Hydro Storage Plant (SPHSP).

Appendix 2: Calculation for the design of SPHSP.

Attachment _1

Volume Estimation for PHS

The volume flow rate of water when turbine operates with 550 MW rated power

$$Q_P = \frac{P_P \times \eta_P}{g \times \rho \times h}$$

Where:

Q_P: Rated volume flow rate (m^3/s).

P_P: Rated turbine power (W).

η_P: Pump efficiency.

g: Acceleration of gravity $(9.8\, m/s^2)$.

ρ: Density of water $(1000\, Kg/m^3)$.

h: Head (m).

$$Q_P = \frac{550 \times 0{,}85 \times 10^{\wedge}6}{9{,}8 \times 1000 \times 2000}$$

$$= 23{,}85204 \ m^3/s$$

Assume the turbine works for 3 hours , the required volume of the tank can be estimated by using equation

$$V_R = Q_P \times T$$

Where:

V_R : Volume of the tank

T: Rated pumping time in second

$$V_R = 23{,}85204 \times 3 \times 60 \times 60$$

$$= 257602 \ m^3$$

DESIGN OF SUBSEA PUMP HYDRO STORAGE PLANT

INPUT DATA			
Height of subsea storage tank, H	6800	mm	
Total Width of the Tank	24300	mm	
Width of subsea storage tank, B	6075	mm	(one Segment)
Slab			
Thickness of top slab, t_{ts}	900	mm	
Thickness of bottom slab, t_{bs}	900	mm	
Wall			
Thickness of side walls, t_w	1350	mm	
Thickness of inner walls, t_{w1}	800	mm	
Top of tank from sea surface , h_f	150000	mm	
Concrete unit weight, γ_c	24	kN/m^3	
Water unit weight, γ_s	10	kN/m^3	
Rebar (Fe 500) yield strength, f_y	500	MPA	
Concrete compressive strength, f'_c	50	MPA	
Imposed service dead loads, w_d	0	KPa	
Allowable soil pressure, q_a	250	KPa	
Concrete cover to rebar center	100	mm	
Top Slab Reinforcement	**Top**	**Bottom**	
Rebar size	32	25	
No. of reinforcement layers	2	2	
Main reinforcement spacing	75	75	mm
Bottom Slab Reinforcement	**Top**	**Bottom**	
Rebar size	32	25	
No. of reinforcement layers	2	2	
Main reinforcement spacing	75	75	mm
Wall Reinforcement			
No. of reinforcement layers	2		
Wall rebar size	32	mm	
Wall Main reinforcement spacing	75	mm	
Temperature Reinforcement			
Temperature reinfor	20	mm	
Temperature reinfor. Spacing	300	mm	
Volume Required for Tank	257602,041	m^3	Refer Attachment: 1
Clear Height of tank	5	m	
Clear Width of Tank	20	m	
Clear Length of theTank	5200	m	
Volume Provided	260000		
<u>**Loading**</u>			
Weight of water above top of slab	1500,00	KN/m	
Self weight of the slab	21,6	KN/m	
Pressure at the bottom of the side wall	1568,0	kN/m	
Selweight of walls = t_w (H - t_{bs} - t_{ts}) γ_c	516,0	KN	
Net Buoyancy	68,0	kN/m	
Pressure due to stru. selfweight	1496,43	kN/m	
FACTORED LOAD			
Load factor for dead load	1,5		
Load factor for horizontal earth pressure	1,5		

Sea Surface

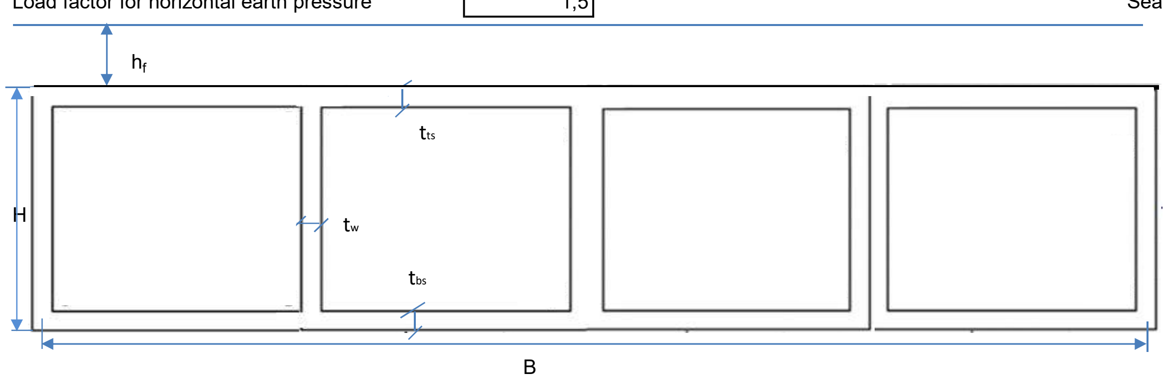

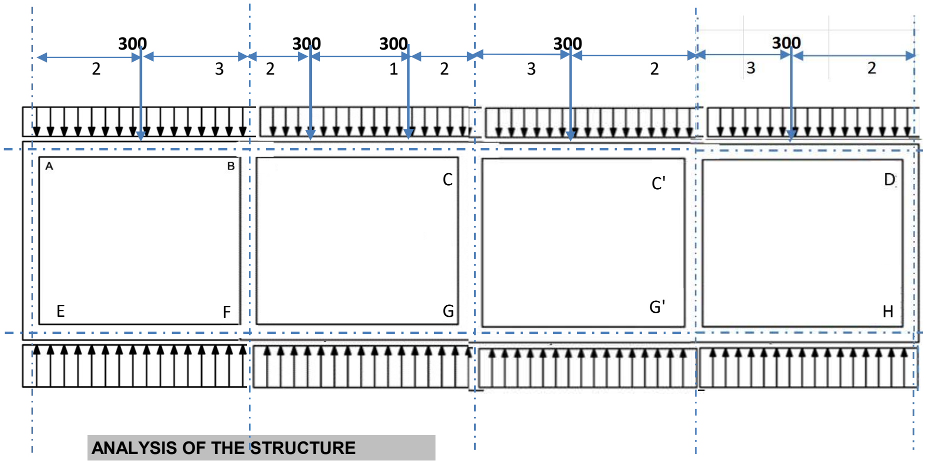

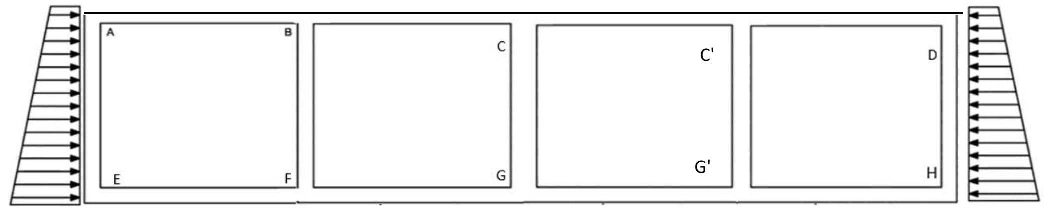

ANALYSIS OF THE STRUCTURE

The structure is analyzed using the moment distribution method.

The fixed-end moment at each joint is the superposition of the fixed-end moments due to dead, live and earth pressure loads.

Joint	A		B			C/C'			D		E		F			G/G'			H	
Member	AE	AB	BA	BF	BC	CB	CG	CD	DC	DH	EA	EF	FE	FB	FG	GF	GC	GH	HG	HD
Length	5,00	5,00	5,00	5,00	5,00	5,00	5,00	5,00	5,00	5,00	5,00	5,00	5,00	5,00	5,00	5,00	5,00	5,00	5,00	5,00
Moment of Inertia	0,2050	0,0608	0,0608	0,2050	0,0608	0,0608	0,2050	0,0608	0,0608	0,2050	0,2050	0,0608	0,0608	0,2050	0,0608	0,0608	0,2050	0,0608	0,0608	0,2050
I/L	0,0410	0,0122	0,0122	0,0410	0,0122	0,0122	0,0410	0,0122	0,0122	0,0410	0,0410	0,0122	0,0122	0,0410	0,0122	0,0122	0,0410	0,0122	0,0122	0,0410
Distrib. Factor	0,77	0,23	0,19	0,63	0,19	0,19	0,63	0,19	0,23	0,77	0,77	0,23	0,19	0,63	0,19	0,19	0,63	0,19	0,23	0,77
FEM	4772,50	-4971,00	4899,00	0,00	-5115,00	5115,00	0,00	-4899,00	4971,00	-4772,50	-4815,00	4676,36	-4676,36	0,00	4676,36	-4676,36	0,00	4676,36	-4676,36	4815,00
Balance	-198,50		-216,00			216,00			198,50		-138,64		0,00			0,00			138,64	
Distribution	153,13	45,37	40,19	135,63	40,19	-40,19	-135,63	-40,19	-45,37	-153,13	106,95	31,69	0,00	0,00	0,00	0,00	0,00	0,00	-31,69	-106,95
Carry Over	53,48	20,09	22,69	0,00	-20,09	20,09	0,00	-22,69	-20,09	-53,48	76,56	0,00	15,84	67,81	0,00	0,00	-67,81	-15,84	0,00	-76,56
Balance	73,57		2,59			-2,59			-73,57		76,56		83,66			-83,66			-76,56	
Distribution	-56,75	-16,82	-0,48	-1,63	-0,48	0,48	1,63	0,48	16,82	56,75	-59,06	-17,50	-15,56	-52,53	-15,56	15,56	52,53	15,56	17,50	59,06
Carry Over	-29,53	-0,24	-8,41	-26,26	0,24	-0,24	26,26	8,41	0,24	29,53	-28,38	-7,78	-8,75	-0,81	7,78	-7,78	0,81	8,75	7,78	28,38
Balance	-29,77		-34,43			34,43			29,77		-36,16		-1,78			1,78			36,16	
Distribution	22,97	6,81	6,41	21,62	6,41	-6,41	-21,62	-6,41	-6,81	-22,97	27,89	8,26	0,33	1,12	0,33	-0,33	-1,12	-0,33	-8,26	-27,89
Carry Over	13,95	3,20	3,40	0,56	-3,20	3,20	-0,56	-3,40	-3,20	-13,95	11,48	0,17	4,13	10,81	-0,17	0,17	-10,81	-4,13	-0,17	-11,48
Balance	17,15		0,76			-0,76			-17,15		11,65		14,78			-14,78			-11,65	
Distribution	-13,23	-3,92	-0,14	-0,48	-0,14	0,14	0,48	0,14	3,92	13,23	-8,99	-2,66	-2,75	-9,28	-2,75	2,75	9,28	2,75	2,66	8,99
Carry Over	-4,49	-0,07	-1,96	-4,64	0,07	-0,07	4,64	1,96	0,07	4,49	-6,61	-1,37	-1,33	-0,24	1,37	-1,37	0,24	1,33	1,37	6,61
Balance	-4,56		-6,53			6,53			4,56		-7,99		-0,20			0,20			7,99	
Distribution	3,52	1,04	1,21	4,10	1,21	-1,21	-4,10	-1,21	-1,04	-3,52	6,16	1,83	0,04	0,12	0,04	-0,04	-0,12	-0,04	-1,83	-6,16
Carry Over	3,08	0,61	0,52	0,06	-0,61	0,61	-0,06	-0,52	-0,61	-3,08	1,76	0,02	0,91	2,05	-0,02	0,02	-2,05	-0,91	-0,02	-1,76
Balance	3,69		-0,02			0,02			-3,69		1,78		2,94			-2,94			-1,78	
Distribution	-2,85	-0,84	0,00	0,02	0,00	0,00	-0,02	0,00	0,84	2,85	-1,37	-0,41	-0,55	-1,85	-0,55	0,55	1,85	0,55	0,41	1,37
Carry Over	-0,69	0,00	-0,42	-0,92	0,00	0,00	0,92	0,42	0,00	0,69	-1,42	-0,27	-0,20	0,01	0,27	-0,27	-0,01	0,20	0,27	1,42
Balance	-0,68		-1,35			1,35			0,68		-1,70		0,08			-0,08			1,70	
Distribution	0,53	0,16	0,25	0,85	0,25	-0,25	-0,85	-0,25	-0,16	-0,53	1,31	0,39	-0,01	-0,05	-0,01	0,01	0,05	0,01	-0,39	-1,31
Moment Sum	4915,61	-4915,61	4962,26	128,90	-5091,16	5091,16	-128,90	-4962,26	4915,61	-4915,61	-4688,71	4688,71	-4684,26	17,16	4667,10	-4667,10	-17,16	4684,26	-4688,71	4688,71

SHEAR MOMENT DIAGRAMS

Top Slab

Forces for Top Slab			
Length		6,08	
Reaction		6932,79	
Interval		0,30	
Unit wt on top slab		2282,40	
Moment(Mab)		-4915,61	
Moment(Mba)		4962,26	
Index No.	**X**	**M**	**V**
0	0,00	-6239	6933
1	0,30	-4239	6240
2	0,61	-2449	5546
3	0,91	-869	4853
4	1,22	499	4160
5	1,52	1658	3466
6	1,82	2605	2773
7	2,13	3342	2080
8	2,43	3869	1387
9	2,73	4185	693
10	3,04	4290	0
11	3,34	4185	-693
12	3,65	3869	-1387
13	3,95	3342	-2080
14	4,25	2605	-2773
15	4,56	1658	-3466
16	4,86	499	-4160
17	5,16	-869	-4853
18	5,47	-2449	-5546
19	5,77	-4239	-6240
20	6,08	-6239	-6933

Top Slab Moment Diagram

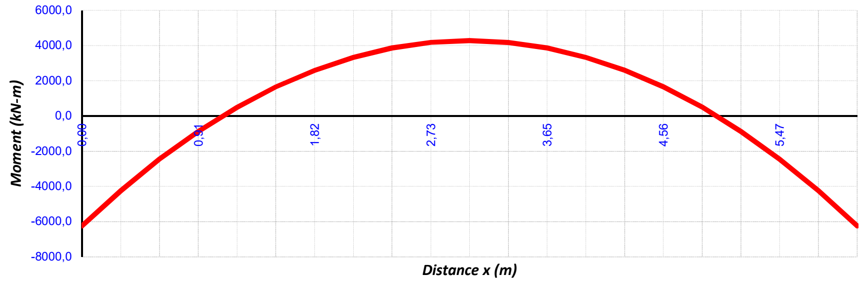

$M_{max\ (+)}$	4290	kN/m
$M_{max\ (-)}$	-6239	kN/m
Design Moment	6239	kN/m

Top Slab Shear Diagram

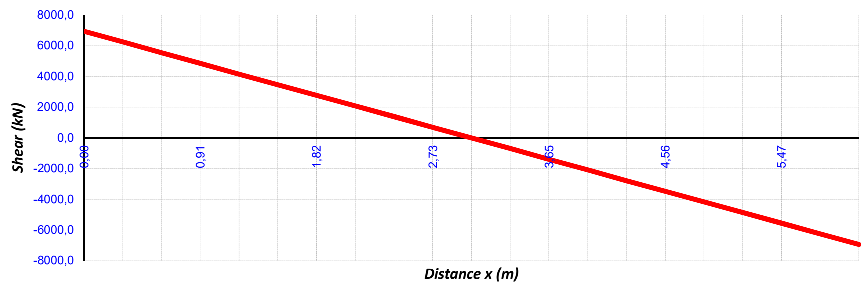

$V_{max\ (+)}$	6933	kN
$V_{max\ (-)}$	-6240	kN
Design Shear	2026	kN

At distance d from the face of the support

Bottom Slab

Forces for Bottom Slab			
Length		6,075	
Reaction		6818,13	
Interval		0,30375	
Unit wt on top slab		2244,652	
Moment(Mef)		4688,71	
Moment(Mfe)		-4684,26	
Index No.	**X**	**M**	**V**
0	0,00	6148	-6818
1	0,30	4180	-6136
2	0,61	2420	-5455
3	0,91	867	-4773
4	1,22	-480	-4091
5	1,52	-1619	-3409
6	1,82	-2551	-2727
7	2,13	-3275	-2045
8	2,43	-3793	-1364
9	2,73	-4104	-682
10	3,04	-4207	0

Bottom Slab Moment Diagram

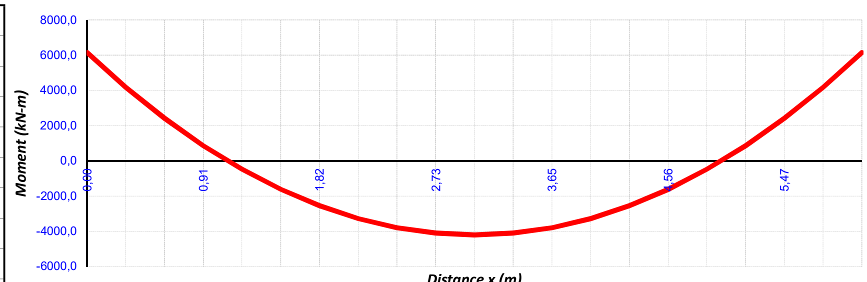

$M_{max\ (+)}$	6148	kN/m
$M_{max\ (-)}$	-4207	kN/m
Design Moment	6148	kN/m

11	3,34	-4104	682
12	3,65	-3793	1364
13	3,95	-3275	2045
14	4,25	-2551	2727
15	4,56	-1619	3409
16	4,86	-480	4091
17	5,16	867	4773
18	5,47	2420	5455
19	5,77	4180	6136
20	6,08	6148	6818

Bottom Slab Shear Diagram

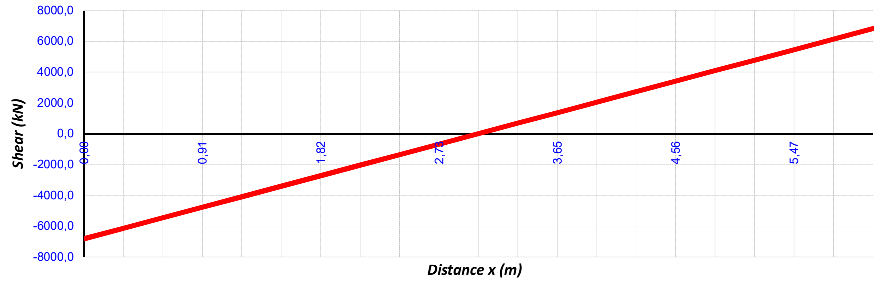

$V_{max\ (+)}$	6818	kN
$V_{max\ (-)}$	-6818	kN
Design Shear	1992	kN

At distance d from the face of the support

Side Walls

Forces for side wall			
Length	5		
Reaction	3317,635		
Interval	0,25		
	wmax	2352	
	wmin	2250	
Moment(Mae)	4915,61		
Moment(Mfe)	-4688,71		
Index No.	**X**	**M**	**V**
0	0	6148	3318
1	0,25	6927	3012
2	0,5	7607	2707
3	0,75	8187	2403
4	1	8668	2101
5	1,25	9050	1800
6	1,5	9333	1500
7	1,75	9519	1202
8	2	9606	904
9	2,25	9596	609
10	2,5	9489	314
11	2,75	9284	21
12	3	8983	-272
13	3,25	8586	-562
14	3,5	8093	-852
15	3,75	7504	-1140
16	4	6820	-1427
17	4,25	6041	-1713
18	4,5	5167	-1997
19	4,75	4198	-2280
20	5	3136	-2562

Side Walls Moment Diagram

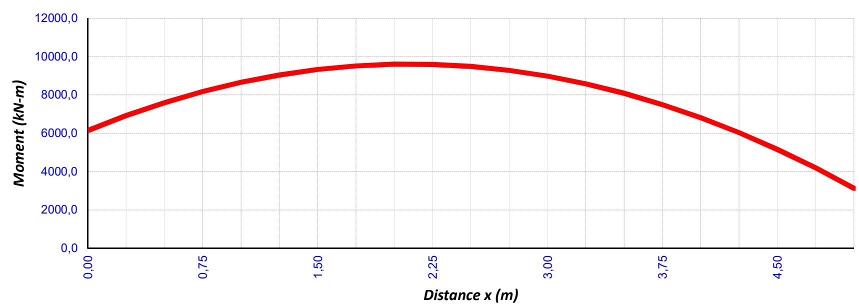

$M_{max\ (+)}$	9606	kN/m
$M_{max\ (-)}$	3136	kN/m
Design Moment	9606	kN/m

Side Walls Shear Diagram

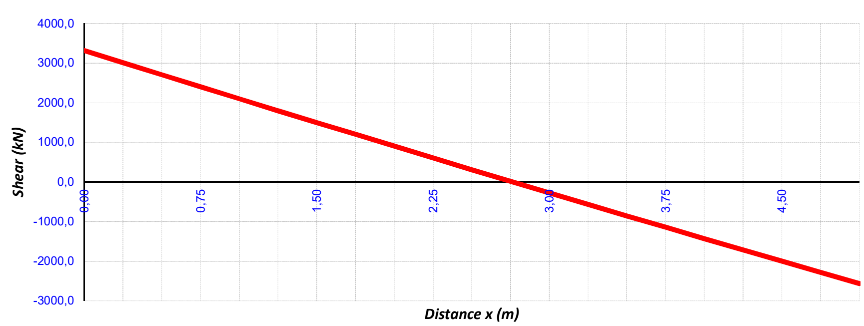

$V_{max\ (+)}$	3318	kN
$V_{max\ (-)}$	-2562	kN
Design Shear	727	kN

At distance d from the face of the support subsea 7 TUDelft

SHEAR STRENGTH CHECK

Nominal Shear Stress τ_v = $\frac{V_u}{bd}$

Percentage of Tension Reinforcement (P_t %) = $\frac{Ast \times 100}{bd}$

Design Shear Strength of Concrete τ_c corresponding to Nominal Shear Stress and percentage of Tension reinforcement. Refer P.73 table 19 of IS 456 200

If τ_v < τ_c No Shear reinforcement required

If τ_v > τ_c Shear Reinforcement required in the form of stirrups

Spacing of Stirrups Sv = $\frac{0.87 \times fy \times Asv \times d}{Vus}$

Vus = $Vu-\tau_c x b x d$

V_u = Factored Shear force

b = breadth of wall/slab = 1000 mm

d = Thickness of wall/slab

A_{sv} = Area of the stirrups

Component	d (mm)	V_d (kN)	$\tau_v = V_d/bd$	τc max(N/mm^2)	% of Steel	τc Permis.		Vus =Vu-tc*b*d	Spacing
Top slab	800	2025,6	2,53	4,5	2,4	0,94	Not ok	1273630	71
Bottom slab	800	1992,1	2,49	4,5	2,4	0,94	Not ok	1240129	73
Side walls	1250	726,7	0,58	4,5	1,6	0,82	ok	0	0

REINF. CALCULATIONS

Component		MAIN REINFORCEMENT						Temperature Reinforcement
		d (mm)	M_u(kN-m)	A_s (mm^2)	$A_{s\ prov}$	ρ_{act}	Status	
Top slab	Top	800	6239,2	17331	21447	2,4	O.K.	0,12 % of Total Cross Section
	Bottom	800	4290,0	11917	13090	1,5	O.K.	
Bottom slab	Top	800	6147,6	17077	21447	2,4	O.K.	
	Bottom	800	4207,4	11687	13090	1,5	O.K.	
Side walls		1250	9606,1	17078	21447	1,6	O.K.	

CONCRETE VOLUME CALCULATION			
WALL			
		Wall outer	Wall inner
Length	m	5200	5200
Thickness	m	1,35	0,8
height	m	2,5	2,5
Volume	m^3	8775,00	5200
SLAB			
		Slab Bott	Slab Top
Length	m	5200	5200
Thickness	m	0,9	0,9
Width	m	24,3	24,3
Volume	m^3	113724	113724
Total	m^3	241423	

REINFORCEMENT QUANTITY CALCULATION

SLAB

Number of Main bars in Transverse direction	=	87333	
No. of layers	=	2	
Width	=	24,3	
Top Bars total length	=	2122200	m
Bottom Bars total length	=	2122200	m
Temp Reinforcement	=		
Number of bars in Longitudinal direction	=	81	
Number of bars in Longitudinal direction (Bottom)		81	
Top Bars total length	=	530550	m
Bottom Bars total length	=	530550	m
Total weight of Bars	=	29425031	kg

WALL		Exterior	Interior	
Number of Bars in Vertical Direction	=	87333	87333	
layers	=	2	2	
width	=	3	3	m
Bars total length	=	873333	873333,3333	m
Temp Reinforcement	=			
Number of bars in Longitudinal direction	=	8		
Bars total length	=	218333		
Total weight of Bars	=	11570407		

Total			Unit Price($)/ kg	
Concrete	=	241423	57	13761111
Reinforcement	=	40995437	0,58	23777354
TOTAL COST =				37538465